AD A145 879 ABSTRACTS OF PAPERS PRESENTED AT THE ANNUAL MEETING OF 1/1
THE SOCIETY OF GEN..(U) EMORY UNIV ATLANTA GA DEPT OF
PHYSIOLOGY 09 SEP 84 N00014-84-G-0110

UNCLASSIFIED F/G 6/16 NL

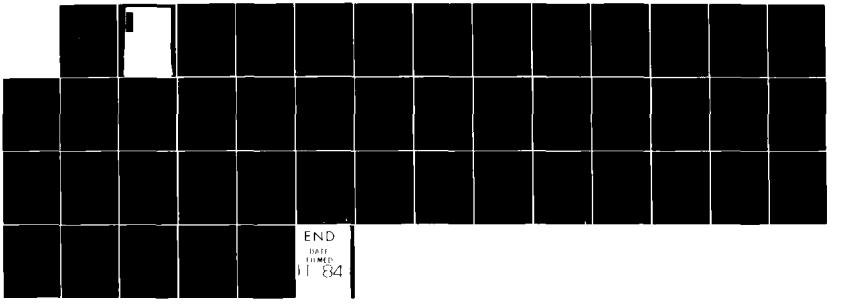

END
DATE FILMED
11 84

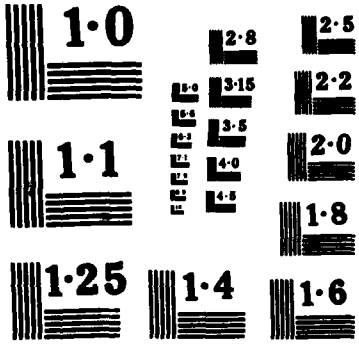
1·0
1·1
1·25
2·8
3·15
3·5
4·0
4·5
1·4
2·5
2·2
2·0
1·8
1·6

SOCIETY OF GENERAL PHYSIOLOGISTS

Robert B. Gunn, M.D., Treasurer
Department of Physiology
Emory University
School of Medicine
Atlanta GA 30322

September 13, 1984

ACO
Office of Naval Research Resident
Representative
Georgia Institute of Technology
206 O'Keefe Building
Atlanta, Georgia 30332

Dear Sir:

Enclosed are copies of the Proceedings of the Symposium on Opitcal Methods in Cell Physiology held in Woods Hole, MA on September 6-9, 1984 and supported, in part, by Grant No: N00014-84-G-0110.

These are submitted in fulfillment of the grant above.

Sincerely,

Robert B. Gunn, M.D.
Treasurer
SGP

RBG:ph

Enclosures

ABSTRACTS OF PAPERS PRESENTED AT THE THIRTY-EIGHTH ANNUAL MEETING OF THE SOCIETY OF GENERAL PHYSIOLOGISTS

Marine Biological Laboratory

Woods Hole, Massachusetts

6–9 September 1984

INVITED PAPERS

1. Advances in Video-enhanced Microscopy ROBERT DAY ALLEN, *Department of Biology, Dartmouth College, Hanover, New Hampshire*

The AVEC methods of videomicroscopy have provided biomedical and materials science researchers with light microscopic images of unparalleled contrast, sufficient to detect structures and biological processes well below the accepted limit of spatial resolution (Allen, R. D., and N. S. Allen, 1983, *J. Microsc.*, 129:3). In collaboration with the staff of Hamamatsu Photonics, K. K., and Carl Zeiss/Oberkochen, we have developed a photonic microscope system consisting of a modified Zeiss AXIOMAT microscope and the H.P.K.K. C-1966 Image Processor. The latter contains analog enhancement (U.S. Patent 4,412,246) and hard-wired digital image processing equipment designed specifically to carry out the operations necessary not only for the AVEC methods of polarized light and DIC enhancement, but to enhance by similar operations all of the other classical modes of optical microscopy, including phase contrast and various types of anaxial illumination. The photonic microscope system has been designed to achieve the optimum performance possible with the light microscope using both conventional contrasting and AVEC methods. The photonic microscope system is designed also to achieve one of the long-cherished goals of quantitative microscopy: the generation of images in which contrast is proportional to a single optical property exclusive of all others. By phase-modulating the state of polarization in adjacent video frames and manipulating these images arithmetically, the bright-field contrast (absorption, scattering, refraction) can be removed, and contrast caused by birefringence, optical rotation, or linear or circular dichroism can be viewed selectively at very high sensitivity. Optical path differences or gradients in the optical path can also be viewed selectively by phase-modulating the state of polarization in a double-beam or differential interference microscope. Some examples will be shown of cellular details and processes that could never have been revealed by conventional microscopy or photomicrography.

2. Computer-aided Light Microscopy SHINYA INOUÉ, GORDON W. ELLIS, and THEODORE INOUÉ, *Marine Biological Laboratory, Woods Hole, Massachusetts; University of Pennsylvania, Philadelphia, Pennsylvania; Universal Imaging Corp., Falmouth, Massachusetts*

Ultimately, light microscopy of living cells is limited by the wavelength of the imaging light, by the number of signal photons received per unit image area per unit time, and by the ratio between the number of signal photons received and the noise (nonsignal photons and detector-generated noise) received in the same interval and area. The wavelengths that are usable are set by the susceptibilities of the cells examined as well as by the detector characteristics. The number of photons received per unit area and time is a function of both the illumination intensity and the collection efficiency of the optics, and maximization requires the optics to be both well corrected and of maximal effective aperture. Nonsignal photons are a consequence of the practical limitations of the optical imaging process. Their relative number depends also on the optical methods use for contrast enhancement. The use of image-intensifying video cameras improves the visibility and contrast of the image of low light level objects at the cost of a relative degradation of image definition. No type of camera can recover image information that was not captured by the optics and no type of signal processing can recover information that was not present in the signal transmitted by the camera, but the intelligibility of that information can be vastly improved by appropriate processing. This is seen dramatically with intensified images. We report here on the new, relatively low cost, microprocessor-controlled image-processing boards now available and on the software that enables their use for image summing and averaging, contrast manipulation and enhancement, including pseudocolor renditions and background subtraction, all on real-time video images, and on a variety of image

evaluations and enhancements, including pixel intensity histograms and image convolution, performed in seconds on stored images. The significance of this report lies less in the fact that these image operations can be performed than in the fact that they can now be performed with equipment no more expensive than many research microscopes.

3. Techniques for the Study of Cell Shape WALTER W. STEWART, *National Institute of Arthritis, Diabetes and Digestive and Kidney Diseases, National Institutes of Health, Bethesda, Maryland*

4. Image Intensification of Stained, Functioning, and Growing Cells S. B. KATER, C. S. COHAN, G. A. JACOBS, and J. P. MILLER, *Department of Biology, University of Iowa and Department of Zoology, University of California, Berkeley, California*

The morphology of individual living neurons can be studied to best advantage by either examining them after isolation into cell culture or by injecting them with fluorescent dyes in situ. The major limitation of such approaches is that the light levels generally used for both procedures are deleterious to normal neuronal functioning. The use of visualization methods that are sensitive to ultra-low light levels, however, has circumvented this limitation and has allowed not only the observation of time-dependent changes in neuronal structure but also the experimental evocation of changes in neuronal morphology with subcellular precision. This paper describes the use of silicon intensifier target (SIT) cameras and second-generation microchannel plate image intensifiers for viewing living neurons. These techniques are used (*a*) to identify neurons and their axonal and dendritic arborizations, (*b*) to produce selective axotomy by focal (UV) irradiation, (*c*) to facilitate laser ablation of single dendritic branches, and finally (*d*) to relate specific morphological characteristics with physiological functions (e.g., the spike-initiating zone). These methods provide a unique way to study both normal and plastic properties of neurons. Laser ablation is being used to determine the physiological effects of synaptic inputs that are spatially distributed along a neurite. Focal UV irradiation has been used to produce neurite outgrowth in single neurons by unicellular axotomy. By combining the fluorescent properties of intracellular dyes with the image-intensification techniques mentioned above, it is now possible to study the morphology and connectivity of living neuronal ensembles with a resolution that has not previously been possible.

5. Changes in Molecular Distribution in Cells Revealed by Digital Imaging Microscopy F. S. FAY, *Department of Physiology, University of Massachusetts Medical Center, Worcester, Massachusetts*

Many cellular functions are mediated by changes in the numbers and/or the distribution of molecules and ions within cells. With the development of numerous optical probes for both ions and molecules, the possibility arises of visualizing such changes in single cells. To this end, we have developed a digital imaging microscope that generates a three-dimensional (3D) image of a particular cellular constituent, allowing for interactive quantitative analysis of such changes. This system consists of a conventional light microscope modified so that both the focus mechanism and illumination are under computer control. Images of these ultra-low light levels are acquired with a SIT camera and digitized to 256 gray levels. Images are digitally processed using a microcomputer coupled to an Analogics array processor. The 3D image of the cell is developed from a series of images obtained at 0.25-μm intervals through the depth of the cell. Images at each focal plane consist of several digitized video frames averaged to improve the signal-to-noise ratio and digitally corrected for spatial nonuniformities in camera dark current and gain. Distortions associated with image acquisition are reversed in cellular 3D data by either a linear filter or an iterative restoration technique. The resulting 3D cellular images are often still too complex for analysis, and in such cases we identify a subset of objects of interest within the cell and extract salient features regarding their distribution. This is accomplished by an artificial 3D visual system consisting of several sets of digital filters. Information obtained from the system is used to generate a simplified 3D cellular image that can be viewed in 3D and levels of organization that can be probed by interaction with the 3D display. This approach will be illustrated by an analysis of changes in the distribution of the protein α-actinin during contraction

of smooth muscle. As this protein is believed to be intimately associated with the contractile machinery, changes in its distribution during contraction provide important insights into the mechanism of contraction of smooth muscle. Digital imaging microscopic analysis of α-actinin distribution has revealed that this protein is found in discrete bodies organized into a mat-like cable, anchored at points along the cell membrane, consisting of strings that are composed of regularly spaced repeating units. It is the distance between these smallest units that diminishes as cells actively shorten, and thus it appears to be the site for force generation. Other applications of digital imaging microscopy will also be discussed. [Supported in part by grants from the NIH (HL14523) and the Muscular Dystrophy Association.]

6. Optical Monitoring of Activity from Buccal Ganglia During Pharyngeal Expansion (Feeding) in a Minimally Dissected *Navanax* L. B. COHEN, J. A. LONDON, and D. ZECEVIC, *Department of Physiology, Yale University School of Medicine, New Haven, Connecticut*

We are investigating the use of optical methods to measure simultaneous action potential activity from many cells in the nervous system of a minimally dissected opisthobranch mollusk, *Navanax inermis*. We hope that the ability to monitor all, or nearly all, of the spike activity in a ganglion while the animal is exhibiting behavior will be useful in helping to determine how the neurons interact to generate the behavior. A modified whole animal preparation was used that allowed the animal's nervous system to be optically monitored during feeding. A 1-cm slit was made in the ventral body wall and in the pharynx immediately under the buccal ganglion. One end of a 2.5-cm-long clad quartz rod, used as a light pipe, was pushed through a small hole in the dorsal side of the pharynx and the dorsal body wall and positioned on the stage of a microscope so that it transmitted light from the microscope condenser. The ventral musculature of the pharynx was pinned to a platform at the end of the rod in such a way that one of the buccal hemi-ganglia was positioned over the end of the rod. An enlarged image of the stained ganglion was formed on a 124-element photodiode array. During recording, in order to reduce movement of the ganglion during the vigorous pharyngeal movements, the stage and the ganglion were covered with a 1% agar solution. This reduced the amount of movement artifact, but did not significantly reduce the signal size. The ganglia were stained with a 0.5-mg/ml solution of the symmetrical pyrazo-oxonol dye RH155b, kindly provided by Rina Hildesheim and A. Grinvald. This dye produced the best results of 21 oxonol and merocyanine-rhodanine dyes we tested on *Navanax* ganglia. Action potentials with large signal-to-noise ratios were obtained, while no significant photodynamic damage was observed. Both before and after staining, most animals made spontaneous pharyngeal expansions that were similar to the expansions seen during feeding. An increase in spontaneous pharyngeal expansion rate occurred when a food stimulus was placed on the animal's chemosensory apparatus. Analysis of 20-s recordings of the diode outputs indicated that spike activity in up to eight buccal neurons was detected during expansions. Several different neurons increased their activity during specific phases of the expansion cycle. [Supported by NIH grants NS08437 to L.B.C. and NS-0716901 to J.A.L.]

7. Optical Methods Monitor Action Potentials and Secretory Activity at the Nerve Terminals of Vertebrate Neurohypophyses B. M. SALZBERG, A. L. OBAID, and H. GAINER, *University of Pennsylvania, Philadelphia, Pennsylvania; National Institutes of Health, Bethesda, Maryland; Marine Biological Laboratory, Woods Hole, Massachusetts*

The ability to monitor directly both the secretory events at vertebrate nerve terminals and the local membrane potential changes that regulate them should contribute to our understanding of excitation-secretion coupling. Molecular probes of membrane potential have been used to record the shape of the action potential from populations of synchronously activated neurosecretory terminals in the neurohypophyses of frogs and mice, and to monitor the effects of agents known to influence neuropeptide release. When voltage-sensitive sodium and potassium channels in the frog pars nervosa are blocked with tetrodotoxin and tetraethylammonium, direct field stimulation of the nerve terminals evokes regenerative calcium responses that are sensitive to $[Ca^{++}]_o$ and are reversibly eliminated by the addition of 0.5 mM cadmium chloride.

The neurohypophysis of the mouse (CD-1) exhibits large and rapid changes in opacity, during and immediately after the action potential in its neurosecretory terminals. These optical signals are readily recorded without averaging, and reflect variations in light scattering rather than absorbance. The fractional changes in scattered intensity depend upon the frequency of stimulation and the $[Ca^{++}]_o$, as well as the scattering angle. Some components of the light-scattering change are blocked by Ca^{++} antagonists and are enhanced by known secretagogues; these optical signals appear to monitor an early event in neuropeptide secretion. A different component of the light-scattering signal, approximately coincident with the extrinsic absorption signal provided by voltage-sensitive dyes, appears to reflect the arrival of the impulse in the terminals. Optical measurement of membrane potential, using potentiometric probes, coupled with light-scattering measurements, permit one to monitor simultaneously the voltage changes in mammalian nerve terminals and the release of secretory products. Laser light-scattering experiments should assist in the interpretation of the intrinsic optical signals: the angular dependence of the light-scattering changes may provide important information about the identity of the scatterers, and optical heterodyning may permit the detection of organelle movement with millisecond time resolution. [Supported by USPHS grant NS 16824.]

8. Real-Time Optical Imaging of Neuronal Activity in Mammalian CNS In Vitro and In Vivo

AMIRAM GRINVALD, *Department of Neurobiology, The Weizmann Institute of Science, Rehovot, Israel*

Suitable voltage-sensitive probes were designed and synthesized to facilitate optical monitoring of neuronal activity in mammalian central nervous system (CNS) preparations in vitro and in vivo. The use of an array of photodetectors permits optical recording from hundreds of sites simultaneously. Optical signals are nearly identical in time course to intracellular electrical recording. If a photodetector is positioned over several neuronal elements, then the optical signal represents the average "intracellular population activity." However, such optical signals are restricted to their site of origin, whereas extracellular recording of population activity provides signals that are spread over large, often unpredictable distances. Optical recording has facilitated the investigation of local circuits and the cellular basis underlying the formation of spatiotemporal patterns of neuronal activity in mammalian brain slices (Grinvald et al., 1982, *J. Physiol.* [*Lond.*], 333:269). With the novel probe RH155, such patterns can be recorded without signal averaging. Recently synthesized fluorescent styryl dyes have facilitated optical recording of naturally evoked responses in the somatosensory cortex (Orbach et al., 1983, *Neurosci. Abstr.*, 9:39) and the frog optic tectum (Grinvald et al., 1984, *Nature* [*Lond.*], 308:848). These experiments suggest that optical recording could provide a powerful tool for studying the development, organization, and function of exposed CNS structures in vivo. By means of a computerized optical recording and a display processor, video-displayed images of neuronal elements are superimposed on the corresponding patterns of the optically detected electrical activity, thus allowing the imaging of spatiotemporal pattern of activity. The implementation of existing optical and mathematical approaches that can provide a tomography-like optical imaging of neuronal activity with submillisecond time resolution and 40–60 μm spatial resolution will be discussed.

9. Ionic Transport and the Electrical Properties of Red Cell and Ehrlich Ascites Tumor Cell Membranes Determined with Fluorescent Dyes

JOSEPH F. HOFFMAN and PHILIP C. LARIS, *Department of Physiology, Yale University School of Medicine, New Haven, Connecticut; Department of Biological Sciences, University of California, Santa Barbara, California*

Optical techniques involving the use of fluorescent dyes, such as diS-$C_3(5)$, provide a non-invasive way of estimating membrane potentials of single cells in suspension. The electrical properties of membranes evaluated under a variety of conditions (e.g., changes in ionic composition, metabolic states, presence of transport inhibitors) provide for the analysis of the ionic mechanisms that underlie membrane transport. Thus, measurements of membrane resistance, the effects of membrane potential on anion and cation conductances, and the identification and characterization of electroneutral and electrogenic processes can be carried out. Examples of these types of electrical parameters will be discussed from studies dealing with red blood cells and Ehrlich ascites tumor cells. [Supported by NIH grants HL-09906 and AM-17433.]

10. Acousto-Optical Imaging of Action Potential Spread Over Intact Heart MARTIN MORAD, *Department of Physiology, University of Pennsylvania School of Medicine, Philadelphia, Pennsylvania*

11. Measurement of Calcium Transients in Muscle Using Metallochrome Indicator Dyes W. KNOX CHANDLER, GREG BOYARSKY, MALCOLM IRVING, JAMES MAYLIE, and LEUNG SIZTO, *Yale University, New Haven, Connecticut*

12. Spatial and Temporal Characteristics of Calcium Transients in *Limulus* Photoreceptors JOEL E. BROWN, *Department of Ophthalmology, Washington University, St. Louis, Missouri*

Limulus ventral photoreceptor cells were injected intracellularly with aequorin. Luminescence from intracellular aequorin increased dramatically after stimulation by light. This "aequorin response" both rose more slowly and reached its peak later than the electrical response of the photoreceptor. The aequorin response declined during prolonged stimulation by light to a level higher than the aequorin luminescence in the dark. The aequorin response was present even after calcium ions were chelated out of the extracellular bath. These findings: (*a*) suggest that stimulation induces an increase in intracellular Ca^{++}, at least in part by release from intracellular stores, and (*b*) are consistent with the proposal that Ca^{++} is an intracellular messenger for light adaptation. In separate experiments, arsenazo III was injected into ventral photoreceptors. The absorbance of intracellular dye was measured with a scanning microphotometer in one dimension across the cell body (with a spatial resolution of ~2 μm). Dye absorbance at 580 nm (the isosbestic wavelength for Ca-dye binding) was relatively high across the cell body, which indicated that the dye diffused throughout the cell. Stimulus light induced a delayed increase in the absorbance at 660 nm (an absorbance maximum for Ca-dye binding). This absorbance increase was localized, usually to one or two regions, within the cell body; the absorbance at 660 nm in the remainder of the cell did not change appreciably. These findings indicate that the increase in intracellular Ca^{++} induced by stimulus light is restricted spatially within the photoreceptor, probably to the rhabdomeric lobe of the cell body. This spatial restriction strongly influences the determination of both the amplitude and the kinetics of stimulus-induced changes of intracellular Ca^{++}.

13. Components of Metallochromic Dye Signals from Frog Skeletal Muscle Fibers S. M. BAYLOR, S. HOLLINGWORTH,* M. E. QUINTA-FERREIRA, and C. S. HUI, *Department of Physiology, University of Pennsylvania, Philadelphia, Pennsylvania; Department of Biological Sciences, Purdue University, West Lafayette, Indiana*

The twitch of a skeletal muscle fiber is driven by the rise and fall of the myoplasmic Ca concentration. The myoplasmic [Ca] transient is in turn controlled by the release and re-uptake of Ca from the sarcoplasmic reticulum (SR). In order to study the movement of Ca between SR and myoplasm, intact single twitch fibers from frog (*Rana temporaria*) were mounted on an optical bench apparatus and microinjected with either or both of the metallochromic indicator dyes arsenazo III and antipyrylazo III, and changes in fiber absorbance at wavelengths between 450 and 850 nm were measured in response to action potential stimulation. Several stages of difficulty arise in progressing from the absorbance measurements themselves to inferences about SR Ca movements. First, non-calcium components of the optical signals must be identified, characterized, and removed. Second, the calcium-related absorbance signals must be calibrated in terms of the change in concentration of the Ca-dye complex(es) and also in terms of the underlying change in myoplasmic free [Ca]. Third, the amplitude and time course of the change in myoplasmic total [Ca], which represents the time integral of the net Ca flux (release minus uptake) from the SR, must be estimated from the free [Ca] transient and calculated variations in the occupancy of the major Ca-binding sites accessible to myoplasm. On the basis of a comparison of results obtained with arsenazo III and antipyrylazo III, these various stages of measurement and analysis will be illustrated and discussed. [Supported by NIH grants NS-17620 to S.M.B. and NS-15375 to C.S.H. and an MDA fellowship to S.H.]

Asterisks indicate authors who are not members of The Society of General Physiologists.

14. Intracellularly Trapped Fluorescent pH Indicators JOHN A. THOMAS, *Biochemistry Department, University of South Dakota School of Medicine, Vermillion, South Dakota*

The uncharged diacetate derivatives of fluorescein (F) and 6-carboxyfluorescein (CF) permeate into cells where intracellular esterases release the corresponding fluorescein chromophore. The resultant negatively charged chromophore is retained by the cell, permitting intracellular pH to be determined from the shape of the absorption or fluorescence excitation spectrum. The former method is subject to fewer artifacts, while the latter generally affords greater sensitivity. Calibration curves are constructed from spectral responses observed in various pH buffers after equilibration of the internal and external pH with detergents or ionophores. The spectral signal remaining after centrifugation is used to correct for dye leakage. These dyes are relatively insensitive to their ionic environment, although binding to protein causes long wavelength shifts (vs. buffers) and suppresses the responsiveness to pH. This method has proven successful in both prokaryotic and eukaryotic systems, with the major criteria for success being (*a*) the presence of a suitable intracellular esterase, and (*b*) a reasonably slow rate of dye leakage. F and CF can be used to distinguish pH changes in the mitochondrial and cytoplasmic compartments in whole cells. F behaves intracellularly as a weak acid, concentrating in the most basic compartment, the mitochondrial matrix. Since F has two ionizable protons, a pH gradient of 1 results in distribution ratios approaching 100 in isolated mitochondria. CF, with three ionizable groups, monitors primarily cytoplasmic pH. The esterase reaction releases it initially in the cytoplasm, where it remains, probably because of a low concentration of the permeant, fully protonated species. We are pursuing two methods of using these dyes to quantitate mitochondrial pH gradients in whole cells. Mitochondrial pH can be determined by a combination of CF and DMO measurements. A second method is based on the analysis of the spectral data obtained from the two dyes, using separate calibration curves for the cytoplasmic and mitochondrial compartments.

15. The Design and Intracellular Use of Tetracarboxylate Calcium Indicators ROGER TSIEN, *Department of Physiology-Anatomy, University of California, Berkeley, California*

Calcium indicators can be rationally designed to have high affinities for Ca^{2+}, simple 1:1 stoichiometry, fast kinetics, good rejection of competing cations, and desirable optical properties. These attributes are featured in a family of aryl homologues of EGTA. Unlike previous Ca^{2+} indicators designed for other purposes, they are amenable to a tremendous range of structural variations to fine-tune their molecular characteristics. Another unique advantage is their ease of loading into cells by the action of cytoplasmic esterases on membrane-permeant, labile esters. This method requires no micromanipulations or breaching of the plasma membrane and has thus become a favorite method for populations of small intact cells. Recent progress has produced a second generation of these indicators with up to 25 times stronger fluorescence than their popular predecessor quin 2. This enhancement allows a great reduction in dye loading and added Ca^{2+} buffering. Also, these indicators show major shifts in peak wavelengths, enabling fluorescence ratio detection at two wavelengths to quantify Ca^{2+} with minimal interference from variations in dye content, tissue geometry, or instrumental efficiency. In developing sea urchin embryos, a cell type large enough to have been studied with aequorin and arsenazo III, one of the new dyes gives cleaner and more easily calibrated signals with less toxicity than the previous techniques. Moreover, $[Ca^{2+}]$ measurements with the new dyes can be extended to individual small mammalian cells. Many more variations on the structural theme are possible, as shown by the development of a chelator that changes its Ca^{2+} dissociation constant from ~0.17 to ~7 μM upon illumination. This dye or further homologues should permit spatially and temporally controlled jumps in $[Ca^{2+}]$. More radical structural changes in a different direction can even lead to sodium-selective indicators.

16. Practical Aspects of the Use of Photoproteins as Biological Calcium Indicators JOHN R. BLINKS, *Department of Pharmacology, Mayo Medical School, Rochester, Minnesota*

Photoproteins have now been used as intracellular Ca^{++} indicators in more than 50 types of living cells with little evidence of toxicity. Their outstanding advantage over other indicators is

their relative immunity to motion artifacts. This makes them particularly attractive for studies of the Ca^{++} transients of contracting muscle, and they are the onlv Ca^{++} indicators so far to have been used successfully for this purpose in cardiac muscle. A disadvantage of the photoproteins is their inability to follow very rapid Ca^{++} transients without distortion. Obelin responds more rapidly than aequorin and may be preferable in some circumstances for this reason. It is also somewhat less sensitive to Ca^{++} than aequorin. When aequorin has been pre-equilibrated with physiological concentrations of Mg^{++}, its response to rapid changes in $[Ca^{++}]$ is considerably slower than when it is exposed simultaneously to Ca^{++} and Mg^{++} (E. D. W. Moore, this meeting). Thus, under physiological conditions, the response of aequorin (and presumably of other photoproteins) is slower than previously thought. Another feature of photoproteins that is sometimes troublesome (and sometimes advantageous) is the steepness of their Ca^{++} concentration-effect curves. The curve for acetylated aequorin (Shimomura and Shimomura, 1982, *FEBS Lett.*, 138:201) is less steep, but the relation between $[Ca^{++}]$ and light emission is still far from linear (Moore et al., this meeting). In the presence of 3 mM Mg^{++}, acetylated aequorin responds more slowly than native aequorin. A potential advantage of acetylated aequorin is that its Ca^{++}-independent luminescence is considerably higher than that of native aequorin. Thus, the light signal from a cell containing a small amount of aequorin will be easier to detect above the noise of the photomultiplier when acetylated aequorin is used. One difficulty in the use of photoproteins has been the need for microinjection to introduce them into cells. Several alternative methods are now available, all of which depend on temporary disruption of the surface membrane. [Supported by USPHS grant HL 12186.]

17. The Use of Quin 2 as an Intracellular Ca Indicator in Single Cells and Small Cell Assemblies

J. I. KORENBROT and J. E. BROWN, *Department of Physiology, University of California, San Francisco, California; Department of Ophthalmology, Washington University, St. Louis, Missouri*

Quin 2 is a Ca-selective fluorescent indicator that can be loaded into cells through the use of its hydrophobic acetoxymethyl (AM) ester. This indicator has been successfully used to measure intracellular Ca under experimental conditions in which the fluorescence of a large number of cells (10^6–10^8 cells/ml) in relatively large volumes (1–4 ml) is measured. We have investigated its usefulness in single cell measurements and in spatially resolved measurements of small numbers of cells. The technical requirements of these measurements are demanding because in addition to the need for microscopic image resolution, the quantum yield of fluorescence of quin 2 is relatively small and the difference in quantum yield between the Ca-free and Ca-bound forms is only ~5. We attempted to use quin 2 in single photoreceptor cells of the *Limulus* ventral eye, cells that are known to exhibit light-dependent changes in intracellular Ca. The presence of quin 2 was tested both electrophysiologically and microfluorometrically. We failed to load cells with quin 2 following incubation in AM-quin, although the cells can enzymatically remove the AM groups, as proven by the successful loading of BAPTA, a Ca buffer, following incubation in AM-BAPTA. Cells could be loaded with quin 2 by microinjection. Surprisingly, the cells appeared to contain free quin 2 in their cytoplasm only transiently after the microinjection. Quin 2 in the cytoplasm can apparently be rapidly sequestered or compartmentalized. To measure the spatially resolved fluorescence of a small number of cells, we constructed a novel instrument and measured the fluorescence of rod outer segments in 100-μm-thick toad retina slices. The rod outer segment can be loaded with quin 2 without cell damage only after careful incubation in an aerated, enriched culture medium. The cytoplasmic quin 2 acts as an effective Ca buffer and its presence can be detected electrophysiologically as well as microfluorometrically.

18. Strategies for the Selective Measurement of [Ca] in Various Regions of the Squid Axon

L. J. MULLINS, *Department of Biophysics, University of Maryland School of Medicine, Baltimore, Maryland*

It has become apparent that because of intracellular Ca buffering, the rate of movement of Ca inside a cell is quite slow; hence, measurements of $[Ca]_i$ are often limited to a very local region. We have used several optically based arrangements for the measurement of $[Ca]_i$ and these are detailed below. First, one can confine the Ca-sensitive photoprotein aequorin to a plastic dialysis capillary and position this capillary close to the center of a squid giant axon. The

region of measurement is now some 200 μm from the axon surface membrane and the measurements that can be made with this arrangement will be shown in detail. They indicate a $[Ca]_i$ of ~20–30 nM and a half-time of ~30 min for a $[Ca]_i$ rise when a step change in $[Ca]_o$ is made at the surface. Second, the region of measurement can be limited to one very close to the surface of the axon by injection of not only aequorin, but also of phenol red in concentrations of the order of 100 mM. Calculation suggests that the blue light emission of aequorin is highly absorbed over path lengths of 200 μm, and that one is sampling from the first 20 μm of axoplasm in terms of the light emission of aequorin. While light emission is at the limits of detection, measurements suggest that Ca entry is handled in ways that are different from those detailed above: there is no measurable response to stimulation unless CN^- is present, and responses to increases in Ca influx occur with half-times of seconds. Third, it is possible to inject aequorin into a squid giant axon and to make measurements that are a combination of those detailed above. Most of the aequorin response in such axons is the result of the surface entry of Ca, and measurements of this light emission can be related to actual Ca entry. The measurements detailed above have been compared with Ca entry as measured with arsenazo III and, therefore, some correction of the Ca entry as measured with aequorin is possible.

19. Design and Application of Photolabile Intracellular Probes JEANNE M. NERBONNE, *Division of Biology, California Institute of Technology, Pasadena, California*

Light-sensitive protecting groups, in particular the *o*-nitrobenzyl moiety, are being exploited in several laboratories in the development of photolabile bioactive molecules. The goal is to prepare physiologically inert precursors that are thermally stable and photolabile; irradiation yields the molecule of interest. Using this approach, "concentration jumps" can be made in cells under physiological investigation with spatial and temporal resolution unmatched by conventional techniques. To study directly the structural features affecting the rates and efficiencies of photorelease, a series of *o*-nitrobenyl esters was prepared. We find that although the reaction rates vary slightly with pH or leaving group, large effects accompany changes in chromophore structure: substitution on the ring can alter rates >200-fold. Similarly, thermal and optical properties can be controlled structurally. Photorelease is efficient (quantum yields 0.35–0.90) for all compounds examined and is little affected by structural modifications. As a result of these studies, generally useful photolabile protecting groups have been designed, and photoactivatable proton donors and cyclic nucleotides have been prepared and used. In voltage clamped frog atrial trabeculae, cAMP jumps increase the amplitudes of the slow inward Ca^{++} current (I_{si}) and twitch tension; cGMP jumps have no effects. The kinetics and the voltage dependencies of I_{si} and tension are unaltered by cAMP. The magnitude of the increase, the time to peak response, and the recovery time vary with the amplitude of the cAMP jump produced. Following single flashes, increases can be detected in 150–200 ms, although full effects require 10–30 s for completion (cAMP is released in <5 ms). In the presence of the light-sensitive Ca^{++} antagonist nifedipine, flash effects, in contrast, are complete within 10 ms. In whole cell recordings from cultured rat ventricular myocytes, I_{si} similarly recovered within several milliseconds after photoremoval of nifedipine. The mechanistic implications of these results and the overall potential of this approach, in mechanistic studies, particularly when applied in conjunction with the whole cell patch clamp recording technique, will be discussed. [Supported by the American Heart Association and NIH grant GM-29836.]

20. Mechanisms of Fast Membrane Potential-sensitive Dyes ALAN WAGGONER, *Department of Biological Sciences and Center for Fluorescence Research in the Biomedical Sciences, Carnegie-Mellon University, Pittsburgh, Pennsylvania*

Action potentials of excitable cells produce changes in the electric field strength within the lipid region of membranes of $>10^5$ V/cm. It is not surprising that such large electric field changes can cause significant translation of charged molecules and rotation of dipolar molecules within the membrane. For example, the light absorption and fluorescence signals from axons stained with merocyanine 540 occur as a result of potential-dependent rotation of dipolar dye molecules in the membrane. The rotation affects the relative populations of merocyanine 540 monomers, which are highly fluorescent, and dimers, which absorb light in a different region of the spectrum and are nonfluorescent. It has been proposed that another class of dye molecules, the impermeant oxonols of which WW781 is a member, respond to membrane potential changes

by a different mechanism that does not include dimers. There is evidence that the dye molecules are driven by potential changes between two different solvent environments. Optical signals arise because the absorption spectra of the dye are different in the two solvent environments. Details of these two mechanisms will be discussed and compared with the mechanisms that have been proposed for other potential-sensitive dyes.

21. Membrane Dynamics Studied by Fluorescence Correlation Spectroscopy and Photobleaching Recovery ELLIOT E. ELSON,* *Department of Biological Chemistry, Washington University School of Medicine, St. Louis, Missouri*

Fluorescence correlation spectroscopy (FCS) and fluorescence photobleaching recovery (FPR) are closely related methods for measuring rates of transport and chemical reactions. FPR and FCS share a common simple conceptual basis. The numbers of molecules of specified types in a defined open observation volume are measured as functions of time via their fluorescence. Molecules of a component can appear or disappear either by being created or destroyed in chemical reactions or by diffusing into or out of the volume. Hence, the rate of change of the concentration of the reactant is determined by the rates both of diffusion and of chemical reaction. Therefore, by measuring rates of concentration change, one can obtain both chemical rate constants and transport coefficients. A fundamental distinction between FCS and FPR is that the former is based on measurement of the spontaneous microscopic concentration fluctuations that occur in the system as it rests in thermodynamic equilibrium, while FPR measures the relaxation of a macroscopic spatial gradient in concentration produced by local photolysis. In an FCS measurement, conventional phenomenological rate coefficients must be obtained by statistical analysis of many observed fluctuations. In contrast, FPR yields the desired coefficients from the record of a single relaxation transient. Therefore, FCS is less useful for studies of living cells, which typically are not sufficiently stable to permit the observation of a large number of microscopic fluctuations. As a result, almost all studies of cell surface diffusion have been carried out with FPR. On the other hand, FCS enjoys the advantage in principle of not depending on a photolysis process that is usually poorly defined kinetically and photochemically. (The observed recovery process can depend strongly on the mechanism of bleaching.) Furthermore, FCS and FPR provide different ancillary information. FPR indicates the fraction of the labeled fluorophores that are mobile on the time scale of the measurement. FCS can yield an estimate of the state of aggregation of the labeled molecules. During the past decade, FPR measurements on a wide variety of systems have demonstrated that the lateral diffusion of membrane proteins is limited by forces in addition to the viscosity of the membrane lipid bilayer in which they are embedded. The structural basis of these constraints is unknown. In most of these applications, the FPR data have been analyzed in terms of the simple diffusion of one or a few noninteracting fluorescent components. However, a principal interest in the results comes from the information they can provide about the interactions of the diffusing components with the structures that limit their motion. The development of an analytical scheme that takes into account chemical reaction as well as diffusion provides a framework with which to interpret these results. [Supported by NIH grant 30299.]

22. Caged ATP as a Tool in Active Transport Research JACK H. KAPLAN, *Department of Physiology, University of Pennsylvania, Philadelphia, Pennsylvania*

Since the reported synthesis and characterization of caged ATP (Kaplan, Forbush, and Hoffman, 1978), this compound has been used in a variety of studies on muscle contraction and active ion transport. Caged ATP and its analogs caged ADP and caged P_i are esters of a phosphoric acid and 2-nitrophenylethyl alcohol; on photolysis with light at ~340 nm, the free phosphate is released. The initial strategy in using this approach was based on earlier observations that 2-nitrobenzyl esters of carboxylic acids yielded the free acids on photolysis. The properties of caged ATP that make it useful for studies on cellular phenomena are (*a*) hydrolytic stability, (*b*) resistance to hydrolysis by ATPases, and (*c*) the photolability that yields free ATP rapidly with a high quantum yield. Applications of caged ATP (performed in several laboratories) in the study of active transport systems can be divided into three categories: (*a*) studies on partial reactions, e.g., the ATP:ADP exchange of the sodium pump in resealed red cell ghosts, which enabled the characterization of this reaction in a sided intact system; (*b*) structural studies on the Ca pump, where the effects of rapidly added (released) substrate could be observed

without sample disruption; (*c*) the rapid initiation of sodium pump turnover by photoreleased substrate. The success of this approach and the observation that "all aromatics which have a hydrogen ortho to a nitro group will be light sensitive" (Sachs and Hilpert, 1904) make it likely that the aproach can be extended to a variety of photolabile precursors for a great many substrates of interest to cellular physiologists. The chemical pathway for the photocleavage of caged ATP and similar compounds, the information provided by some of the studies performed to date on active transport systems, and the applicability of this approach to other physiological systems will be discussed. [Supported by NIH grant HL30315 and a grant-in-aid from the American Heart Association. J.H.K. is a recipient of RCDA KO4HL01092.]

23. Laser-pulsed Release of ATP and Other Optical Methods in the Study of Muscle Contraction Y. E. GOLDMAN, *Department of Physiology, School of Medicine, University of Pennsylvania, Philadelphia, Pennsylvania*

Two of the outstanding questions in understanding muscle contraction are (*a*) what are the specific relationships between the mechanical and chemical reactions of the cross-bridge cycle? and (*b*) what structural alteration of the myosin head occurs in the cross-bridge power stroke? Photochemical methods have recently enabled progress to be made toward answering the first question. Laser photolysis of caged ATP is a method of introducing ATP into the filament lattice rapidly. The pulse from a frequency-doubled ruby laser lasts 50 ns, during which time caged ATP absorbs 347 nm photons. Approximately half of the excited molecules photolyze into ATP and 2-nitrosoacetophenone with a 10-ms time constant. ATP binds to rigor cross-bridges, and they detach and then enter further cross-bridge cycles at rates monitored by transient tension and stiffness changes. Optical methods have also been used in other labs to probe the second question. The orientation of myosin heads has been studied by observation of polarization of intrinsic protein fluorescence and bound fluorescent and phosphorescent probes. Decay times for fluorescence or phosphorescence polarization relate to the rate of myosin head rotation. Fluorescence energy transfer provides a means to measure distances between two probes. The mechanism of muscle contraction is being elucidated by a combination of optical methods that initiate and monitor specific intermediate reactions of the cross-bridge cycle.

24. Light-Flash Pharmacology: a Review of Time Scales and Mechanisms H. A. LESTER, *Division of Biology, California Institute of Technology, Pasadena, California*

In our experiments, electrophysiological methods are used to monitor the number of active ion channels in a biological membrane while light flashes are used to manipulate intracellular or extracellular molecules that act on these channels. The light-flash method permits either a concentration jump of a photosensitive drug or a direct photochemical perturbation of the ligand-receptor complex. This approach has given useful mechanistic information over a range of time scales covering six orders of magnitude. The fastest events have been seen at the nicotinic acetylcholine receptor of *Electrophorus* electroplaques. A laser flash produces *cis-trans* photoisomerizations of the agonist *trans-Bis*-Q. Channels begin to open or close within 10 μs, which reflects the rapid transfer of information within the receptor protein. The complete relaxations take place on the millisecond time scale of normal channel gating. Channel gating on the millisecond time scale also dominates the reactivation of Ca^{++} channels in heart after photodestruction of nifedipine. A few milliseconds are required for blockade of ACh channels by a flash-activated "open-channel blocker," but here the rate-limiting step is binding of the blocker to the channel. Tens of milliseconds are involved in the response of nicotinic receptors to concentration jumps of the competitive inhibitor 2BQ; again, the rate constants measure the speed of antagonist binding. It is not clear which step dominates the relatively slow (hundreds of milliseconds) perturbation of muscarinic K^+ channels by concentration jumps of a photoisomerizable competitive inhibitor. Finally, tens of seconds are required for the increases in Ca^{++} currents after an intracellular concentration jump of cAMP; here the rate-limiting step is presumably linked to the phosphorylation of proteins. [Supported by NIH grants NS-11756 and GM-29836, and by the American Heart Association.]

CONTRIBUTED PAPERS

25. Effects of Pre-Equilibration with Mg^{++} on the Kinetics of the Reaction of Aequorin with Ca^{++} EDWIN D. W. MOORE,* *Department of Pharmacology, Mayo Graduate School of Medicine, Rochester, Minnesota* (Sponsor: J. R. Blinks)

Previous studies of the kinetics of the aequorin reaction were done either in the absence of Mg^{++} or under conditions in which the photoprotein was exposed simultaneously to Ca^{++} and Mg^{++}. These conditions might not be appropriate to the use of aequorin as an intracellular Ca^{++} indicator because in the cell the photoprotein is continuously exposed to millimolar concentrations of Mg^{++}. Rapid mixing studies were carried out in a Gibson-type stopped-flow apparatus. The aequorin was dissolved in a Chelex-100-treated solution containing 150 mM KCl and 5 mM PIPES (pH 7.0) with or without 3 mM $MgCl_2$ added, and it was mixed in equal volumes with a similar solution containing 10 mM $CaCl_2$ and enough $MgCl_2$ to make the final $[Mg^{++}]$ 3 mM. The half-time for the rise of luminescence was about doubled when the aequorin had been pre-equilibrated with Mg^{++}, and the rate constant for aequorin consumption in saturating $[Ca^{++}]$ was reduced by ~20%. Pre-equilibration with 3 mM Mg^{++} had an even greater effect on the rise of luminescence of acetylated aequorin, increasing the half-time about fourfold. The effect on the rate of consumption in saturating $[Ca^{++}]$ was similar to that for native aequorin. These results have a number of significant implications. (*a*) They provide strong evidence that aequorin equilibrates with Mg^{++} much more slowly than it does with Ca^{++}. (*b*) They show that under the conditions of the intracellular environment, aequorin responds considerably more slowly to rapid changes of $[Ca^{++}]$ than had been realized and that acetylated aequorin responds even more slowly. (*c*) They reveal that Ca^{++} concentration-effect curves obtained previously by exposing Mg^{++}-free photoproteins to mixtures of Ca^{++} and Mg^{++} were distorted (because there was ample time for equilibration with Mg^{++} at low but not at high $[Ca^{++}]$). [Supported by USPHS grant HL 12186.]

26. Properties of Acetylated Aequorin Relevant to Its Use as an Intracellular Ca^{++} Indicator EDWIN D. W. MOORE,* GARY C. HARRER,* and JOHN R. BLINKS, *Department of Pharmacology, Mayo Graduate School of Medicine, Rochester, Minnesota*

Shimomura and Shimomura (1982, *FEBS Lett.*, 138:201) described methods for acylating Ca^{++}-activated photoproteins, and reported that acetylated aequorin (AA) differed from native aequorin (NA) in a number of potentially important respects. We have used the method they described to prepare AA, extended their observations on its properties, and compared signals recorded from isolated frog skeletal muscle fibers injected with NA or AA. When aequorin is acetylated, the various isoaequorins are no longer readily distinguished by isoelectric focusing. The series of sharp bands that normally focus between pH 4.2 and 4.9 is replaced by a broad blur of luminescent protein between pH 3.6 and 4.4. Acetylation has the following effects on the luminescent reactions. (*a*) For amounts of photoprotein giving equivalent total light yield, the maximum rate of photoprotein consumption (peak light intensity in saturating $[Ca^{++}]$) is reduced by a factor of ~2.5 and the Ca^{++}-independent luminescence is increased by a factor of ~5. (*b*) The slope of the Ca^{++} concentration-effect curve is reduced (to ~1.9 on a log-log plot). (*c*) There is an enhanced effect of Mg^{++}, both on the position of the Ca^{++} concentration-effect curve, and on the rate of rise of luminescence after rapid mixing with Ca^{++} (see E. D. W. Moore, this meeting). In the absence of Mg^{++}, it is possible to detect somewhat lower $[Ca^{++}]$ with AA than with NA. In the presence of 3 mM Mg^{++}, this difference practically disappears, and the response of AA to rapid changes of $[Ca^{++}]$ is significantly slower than that of NA. For a given amount of active photoprotein injected, the "resting glow" from intact muscle fibers is considerably greater for AA than for NA, while the peak luminescence recorded during a twitch is lower with fibers containing AA. [Supported by USPHS grant HL 12186.]

27. Spectrophotometric Determination of Ca, Ba, and AIII Diffusion in Nerve Cell Bodies and In Vitro DOUGLAS TILLOTSON* and ENRICO NASI,* *Department of Physiology, Boston University Medical School, Boston, Massachusetts* (Sponsor: W. Lehman)

A method for estimation of the diffusion rate of ions point-injected into the cytoplasm of single nerve cell bodies is presented. Recordings are made of absorbance changes taking place within a narrow cylindrical region of an *Aplysia* nerve cell that has been filled with arsenazo III (AIII) and is held under voltage clamp. A light-accepting microprobe, fabricated with fused coherent fiber optic and having an accepting tip diameter of ~20 μm, is employed for measurements. A multibarreled microelectrode containing solutions of $CaCl_2$ and $BaCl_2$ is used to administer minute injections of either ion locally, in brief pulses (50 nA, 100 ms), at different distances from the optical beam sampled by a differential microspectrophotometer. Diffusion theory establishes that the diffusion coefficient of the injected ions can be uniquely determined on the basis of the time it takes for the recorded signal to reach a peak, as a function of the distance from the source. Such a measure does not require deriving absolute calcium concentration levels from the absorbance signal or knowledge about the stoichiometry of the Ca-AIII reaction. The only requisite is that the relation between absorbance changes and calcium be linear with respect to calcium concentration (as reported by Palade and Vergara, 1983, *Biophys. J.*, 43:355) and that the calcium concentration be low enough not to saturate the dye at the site of the measurement. This latter condition is easily fulfilled if the injection employed is small and if transients are measured at a sufficient distance from the source. This method has been applied both in vitro and in vivo. Since a significant fraction of calcium is bound to arsenazo, which can undergo diffusion, a theoretical analysis of such a coupled diffusional process is presented that discusses implications for the apparent diffusional rates of the ions under consideration. The effective diffusion coefficient for arsenazo III, uncomplicated by any binding, is directly measured both in vitro as well as in a cell, and the parameter thus obtained is used within our analysis to refine the estimated diffusion coefficients of barium and calcium. [Supported by grant RO1 NS11429-11.]

28. Saturation of Arsenazo III as a Tool to Estimate the Free Calcium Concentration Near the Plasma Membrane Following Stimulation ENRICO NASI* and DOUGLAS TILLOTSON,* *Department of Physiology, Boston University Medical School, Boston, Massachusetts* (Sponsor: J. Saide)

Calcium influx through membrane channels during a voltage clamp step causes large concentration gradients within a nerve cell. This implies that if the cell is injected with the metallochromic dye arsenazo III (AIII), the dye may be saturated in the region just beneath the plasma membrane by the local accumulation of Ca for a short period of time after stimulation. Since the absorbance change recorded is an integrated measure of the total AIII-Ca complex in the volume sampled by the microspectrophotometer, the signal will only reach its maximum value at a time when diffusional redistribution will make the concentration profile of Ca relax below saturating levels, thereby allowing maximum interaction between Ca and AIII. At that moment, the highest concentration, which is at the location of the calcium source, is just below the range where saturation of the dye occurs. If the concentration of AIII in the cell can be determined, then the calcium concentration at the membrane at that time can be empirically estimated by comparison with a suitable titration curve obtained in vitro. This method does not rely on knowing the stoichiometry of the Ca-AIII reaction, and it only requires the assumption that the reaction involved is linear with respect to calcium concentration (although more than one stoichiometric complexes can be formed) and that the stoichiometry does not change with changes in Ca concentration (these assumptions are supported by the results of Palade and Vergara, 1983, *Biophys. J.*, 43:355). Mathematical analysis and computer simulations supporting the validity of this approach are presented. Voltage clamp experiments conducted on *Aplysia giant neurons* reveal that a time lag exists between the offset of a depolarizing step inducing calcium influx and the time at which the arsenazo signal peaks, which suggests that the dye is indeed transiently saturated. This delay is observed to decrease with increase concentration of intracellular AIII, which is consistent with the notion that saturability is decreased under these conditions, while it increases with larger calcium loads. Estimates of lower bounds for the concentration of free calcium that occur at the membrane are presented, and the implications concerning calcium diffusion and buffering are discussed. [Supported by grant RO1 NS11429-11.]

29. Calcium-dependent Absorption Transients Measured with Arsenazo III in Skinned Skeletal Muscle Fibers MICHAEL FILL* and PHILIP M. BEST, *Department of Physiology, University of Illinois, Urbana, Illinois*

The calcium indicator dye arsenazo III (AIII) was used to monitor calcium release from single, skinned (sarcolemma removed) fibers from *Rana temporaria*. Solutions contained (in mM) 100 K propionate, 1 Mg^{2+}, 2 MgATP, 15 creatine phosphate, creatine phosphokinase (15 U/ml), 20 MOPS buffer (pH 7.4, 10°C), $\mu = 0.15$, and variable amounts of EGTA, AIII, and calcium. Calcium release was stimulated by 5 mM caffeine. Absorption was monitored either (*a*) at two wavelengths over long times (several seconds) or (*b*) as complete spectral scans (450–800 nm) taken over 26 ms at various times during a release. Fibers were equilibrated with AIII-containing solutions before stimulation to ensure a constant concentration of dye in the light path during calcium release. The ratio of absorption at 600 compared with 660 nm was ~1.5 and was constant for the first second after stimulation. At longer times, the ratio declined to values approaching 1. The early portion of the absorption transient was fit to a straight line using a least-squares routine. The effect of dye concentration on the slope was determined using a bracketing protocol. Under conditions of maximal loading (60-s exposure to pCa = 5.5), the initial slope increased linearly with dye concentration. In submaximally loaded fibers (15 s), the relationship was nonlinear. Calcium release rates were calculated from the slope of the early absorption changes using a formalism that includes competing buffer systems and dye stoichiometry. Release rates were estimated to be in the range of 1 μM/ms. [Supported by USPHS grant AM 32062 and by a grant from the MDA.]

30. Optical Measurement of Intracellular Free Calcium During Contraction of Single Cardiac Muscle Cells

MICHAEL STUREK,* CHRISTIANE KUTHE,* and KENT HERMSMEYER, *Department of Pharmacology, The Cardiovascular Center, University of Iowa, Iowa City, Iowa*

We have developed a new method for optical measurement of intracellular free calcium or calcium activity ($[Ca^{++}]_i$), using the metallochromic dye arsenazo III (AIII). AIII was loaded into cardiac muscle cells via liposomes, and it was possible to determine changes in $[Ca^{++}]_i$ in 20-μm^2 localized areas of a single cell with the use of interference contrast microscopy and simultaneous dual-wavelength photometry. The reliability of our instrumentation system is indicated by a signal-to-noise ratio of 10:1 when measuring $\Delta[Ca^{++}]_i$-induced changes in absorbance of only 0.004. The problem of movement artifact was corrected by the use of differential wavelength measurements. We specifically found movement artifact to be the same at 580, 660, and 702 nm. Therefore, pure changes in $[Ca^{++}]_i$ could be measured by subtraction of the movement-induced change in absorbance (ΔA) at calcium-insensitive wavelengths (580 or 702 nm) from the ΔA at a wavelength of light (660 nm) where AIII shows a high sensitivity to $[Ca^{++}]_i$. The most novel finding was that the peak $\Delta[Ca^{++}]_i$ in localized areas of the myocardial cell was fivefold greater than the peak $\Delta[Ca^{++}]_i$ from the whole cell. It is unlikely that this optical signal peak could be due to nonuniform AIII concentration within the cell because of measurements at the isosbestic wavelength (580 nm). We hypothesize that this may represent localized release of Ca^{++}, which our calculations suggest might be distributed in only ~20–25% of the cell volume. $[Ca^{++}]_i$ increases in localized areas also occurred on exposure of the myocardial cells to 1 nM norepinephrine, an agent that has been shown by electrophysiological methods to increase calcium inward current in cardiac muscle. In conclusion, the data suggest that Ca^{++}-allowed access to the myofilaments is absorbed, sequestered, or removed rapidly enough that cell buffering is more important than diffusion for the distribution of functionally important $[Ca^{++}]_i$.

31. Difference Spectra Recorded from Voltage Clamped Frog Skeletal Muscle Fibers Injected with Arsenazo III

R. F. RAKOWSKI and MARGARET C. JOST,* *Department of Physiology and Biophysics, Washington University School of Medicine, St. Louis, Missouri*

Differential absorbance spectra were recorded from *Rana temporaria* fast-twitch muscle fibers that were either unstained or injected with the metallochromic indicator dye arsenazo III. The cutaneous pectoris muscle was dissected and placed in a hypertonic solution to prevent contraction. The solution also contained tetrodotoxin (10^{-7} g/ml) to prevent the occurrence of propagated action potentials. Individual muscle fibers were voltage clamped using two intracellular microelectrodes during iontophoretic injection of the dye. Ca^{2+} release was elicited by voltage pulses 105 ms in duration from −80 to 0 mV. A rapid-scanning microscope spectropho-

tometer was used to measure changes in absorbance during and after the depolarizing pulse. A 256-point spectrum could be obtained of wavelengths from 380 to 740 nm at intervals of 7 ms. Both the intrinsic absorbance at rest and the changes in intrinsic absorbance after stimulation of unstained fibers followed a simple wavelength (λ) dependence of λ^{-1}. Fibers injected with arsenazo III that did not release Ca^{2+} upon depolarization gave difference spectra that were similar to the intrinsic absorbance change seen in unstained fibers. Time-resolved differential absorbance spectra obtained in fibers injected with arsenazo III and which gave a characteristic spectral response indicating that Ca^{2+} release had occurred were similar to the peak difference spectra obtained in response to action potential stimulation by Baylor, Chandler, and Marshall 1982, (*J. Physiol.* [*Lond.*]., 331:139). There were two prominent absorbance peaks at 605 and 655 nm and a broad minimum near 500 nm. The peak at 655 nm was greater than the peak at 605 nm. The shape of the spectrum remained approximately constant at all times it could be accurately measured (14–240 ms). The constant shape of the difference spectrum suggests that there is no large change in intracellular pH or $[Mg^{2+}]$ during this period that would interfere with the determination of the time course of Ca^{2+} release, and that the spectrum of the Ca^{2+}-dye response is not significantly affected by the formation of multiple Ca^{2+}-dye complexes.

32. Measurement of Calcium During Fertilization of Sea Urchin Eggs Using a New Fluorescent Indicator M. POENIE, J. ALDERTON, R. STEINHARDT, and R. TSIEN, *Departments of Physiology-Anatomy and Zoology, University of California, Berkeley, California*

We have studied the calcium transient associated with fertilization of *L. pictus* eggs using fura 2, one member of a new family of fluorescent calcium chelators whose excitation spectra change dramatically with calcium. This property has permitted calcium measurements based on fluorescence ratios at two well-separated excitation wavelengths. Eggs were injected with fura 2 because the acetoxymethyl ester was hydrolyzed too slowly to be useful as a method for loading eggs with dye. Excitation wavelengths of 350 and 385 nm were routed from a dual-wavelength, chopping fluorimeter into a Zeiss inverted fluorescence microscope equipped with a photometer. The chopper and photometer outputs were synchronized by computer. Injected eggs gave fluorescent signals 50–100-fold over the background and were capable of cleaving normally through at least the eight-cell stage, which suggests that the procedure was not toxic. The apparent resting level of calcium in unfertilized eggs is 150 nM. During fertilization, calcium rises slowly over a period of 4–6 s and then increases sharply for the next 12–14 s to a peak of 1.8 μM. Free calcium then decays over ~20 min to an average level of 250 nM and never returns to the unfertilized resting level during the first two cleavages. We have monitored changes in fluorescence visually during fertilization looking for a possible "calcium wave," but so far we have seen only uniform changes in fluorescence. There are indications of calcium fluctuations during specific events in the cell cycle, although we have not been able to detect them every time. [Supported by NIH and Searle Scholars Program grants to R.T. and an NSF grant to R.S.]

33. Quin 2 Measurement of Cytosolic Free Ca in Embryonic Chick Heart Cells E. MURPHY, R. JACOB,* A. LEFURGEY, and M. LIEBERMAN, *Department of Physiology, Duke University Medical Center, Durham, North Carolina*

Quin 2 has been used to measure cytosolic free Ca (Ca_f) in various cells. Although quin 2 can qualitatively detect changes in Ca_f, potential problems in quantifying the data are as follows: (*a*) difficulties with the measurement because of extracellular dye and uncertainty of K_D under intracellular conditions and (*b*) alteration of Ca_f by quin 2 loading. Specifically, Ca_f will be overestimated by any quin 2_{ex} that may not be removed by washing. When freshly isolated heart cells were washed just before measuring Ca_f, extracellular quin 2 measured using Mn quenching 1984, (*Fed. Proc.*, 43:767) was 28 ± 2% (± SEM, n = 15). Subsequent incubation of isolated cells (37°C, 30 min) resulted in quin 2 leakage of <10%. However, the $t_{1/2}$ of dye leakage from heart cells in culture was 30 min. Concern that quin 2 might be altering Ca_f came from the following observations. Immediately after loading ($[quin\ 2]_i$ ~ 1 mM), Ca_f (corrected for extracellular dye) averaged 50 ± 4 nM (n = 13), increasing by 44 ± 9% over the first hour. Initially, we attributed this rise in Ca_f to deterioration of the freshly isolated heart cells. However, similar levels of Ca_f were measured on cells isolated at the same time but loaded with

quin 2 as much as 2.5 h apart, and Ca_f rose over a similar time course. Although quin 2 loading could be responsible for the rise in Ca_f, it is unclear whether the initial level of Ca_f was physiological and quin 2 loading caused Ca_f to rise or whether loading depressed Ca_f and the cells gradually recovered to the physiological level. Biochemical and morphological data revealed minimal alterations associated with the loading procedure. Comparing Ca_f by the quin 2 and null point methods (Ca_o nominally zero) resulted in the following: 20 ± 10 nM (quin 2, $n = 4$), 80 ± 70 nM (null point on quin 2 = loaded cells, $n = 4$), and 410 ± 50 nM (null point on unloaded cells, $n = 3$). When cultured heart cells were loaded to ~1 mM [quin 2]$_i$, they became quiescent at about −70 mV. Electrical stimulation produced action potentials followed by afterdepolarizations and eventually spontaneous activity; contractions were feeble or nonexistent. After a short period, the membrane spontaneously returned to the resting state. [Supported by NIH grants HL07101, HL17670, HL27105, HL28280, and HL29687 and by the NC Heart Association.]

34. Cytosolic Free Calcium Levels in the Thick Ascending Limb of Henle's Loop

ELIZABETH MURPHY, MARY E. CHAMBERLIN,* and LAZARO J. MANDEL, *Department of Physiology, Duke University Medical Center, Durham, North Carolina*

A suspension of tubules derived from rabbit medullary thick ascending limbs was prepared by the method described by Chamberlin et al. (1984, *Am. J. Physiol.*). The intracellular free calcium concentration (Ca_f) was measured in this tubule suspension using the dye quin 2. Tubules were incubated with the uncharged form of the dye, quin 2 acetoxymethyl ester (quin-AM) and the fluorescence was monitored. Fluorescence excitation was 340 nm and emission was measured at 450 nm for quin-AM and 510 nm for quin 2. Initially, there was a large fluorescence emission at 450 nm, but this decreased as the intracellular esterases converted quin-AM to quin 2. Concurrently, there was an increase in fluorescence at 510 nm as quin 2 was produced. Ca_f was calculated by correcting for extracellular quin 2 (~30% of the total quin 2 fluorescence) by a method described by Murphy et al. (1984, *Fed. Proc.*, 43:767). Under control conditions, the Ca_f was 99 ± 17 nm ($n = 8$). Ouabain (10^{-4} M) caused no change in the Ca_f. The mitochondrial uncoupler 1799 (10 μM) elevated the Ca_f by 109 ± 45% ($n = 3$) and calcitonin (1 μM) caused a 245 ± 82% ($n = 3$) increase in Ca_f in paired experiments. [Supported by grants from the NIH, the NC Affiliate of the American Heart Association, and the National Kidney Foundation.]

35. Measurement of Free Ca^{+2} Distribution During Mitogenesis Using Quin 2 in Single Living BALB/c 3T3 Cells

F. S. FAY and R. W. TUCKER, *Department of Physiology, University of Massachusetts Medical Center, Worcester, Massachusetts; Johns Hopkins Oncology Center, Baltimore, Maryland*

The role of Ca^{+2} in mitogenesis in mammalian fibroblasts is unclear despite many experiments with cell populations measuring ^{45}Ca fluxes and aequorin luminescence. We propose to test directly the role of free intracellular Ca^{+2} in mitogenesis in quiescent BALB/c 3T3 cells by studying changes in quin 2 fluorescence in single cells. High-resolution images of quin 2 fluorescence are recorded with an ultrasensitive SIT camera and stored in digital form. Sequential frames are averaged to improve the signal-to-noise ratio. Dark current is subtracted from the averaged images. Spatial variations in camera gain and illumination intensity are corrected for by determining a gain factor for each pixel from the response to a uniform field of Ca^{+2}-quin 2. Ca^{+2}-quin 2 fluorescence is uniform throughout the cytoplasm in single cells. Quin 2 fluorescence uniformly (*a*) increases when ionomycin (10 μM) is added to the medium, and (*b*) decreases when EGTA is subsequently added to the medium. The relative contribution of autofluorescence (15–25% of the total fluorescence in a resting cell) and resting intracellular Ca^{+2} (typically 90 μM) is calculated from these measurements plus knowledge of changes in fluorescence in our system of standard quin 2 solutions and Ca^{+2}. We also have found that some growth factors (e.g., platelet-derived growth factor) stimulate a rapid (seconds) threefold increase in quin 2 fluorescence throughout the cell, while other growth factors appear to produce a more localized increase in quin 2 fluorescence. The present results indicate that free Ca^{+2} levels do change early during mitogenesis and that the Ca^{+2} signal may be quite localized within the cell. These issues are now subject to intensive further investigations using these approaches.

[Supported in part by NIH grants HL14523 and CA34472 and by grants from the Muscular Dystrophy Association.]

36. Effect of Extracellular Na^+ and Osmolality on Intracellular Ca^+ in Toad Bladder Cells Measured with Quin 2 HERBERT CHASE, JR. and SHIRLEY WONG,* *Columbia University, New York*

Volume regulation following epithelial cell swelling is thought to result from an increase in basolateral K^+ permeability. Because this requires the presence of extracellular Ca (Ca_o), we examined the effects of swelling on Ca_i using a suspension of toad bladder cells obtained by treating bladders with collagenase and EGTA. After the cells were loaded with quin 2 and washed, fluorescence (f) was measured at 340/480 nm. Ca_i was calculated by obtaining f_{max} with 50 μM digitonin and f_{min} with excess EGTA ([Ca] < 2 nM). The K_d of the dye at a pH of 7.5 was 109 ± 11 nM (n = 4). Ca_i was variable and ranged from 50 to 250 nM (160 ± 16, n = 8). Lowering Ca_o in the presence of A23187 reduced Ca_i to <10 nM, and subsequent addition of 1 mM Ca_o increased Ca_i to > 100 nM. Cyanide, A23187, and gramicidin all increased Ca_i. We studied the effect of swelling by reducing extracellular osmolality (osm_o) with distilled water. Ca_i was 71 nM in cells added to full-strength buffer, and 106 and 114 nM in cells added to ¾- and ½-strength buffer. Because the increase in Ca_i could have been due to the effect of low Na_o, which reduces Na-Ca exchange, rather than to cell swelling, we measured Ca_i after reducing osm_o at a constant Na_o. Ca_i was 176 ± 22 when cells were suspended in a high Na_o buffer, 220 ± 21 when suspended in an isosmotic, low Na_o buffer, and 263 ± 18 when added to a low Na_o, hypotonic buffer. In other experiments, we found that the increase in Ca_i was prevented when cells were diluted into an EGTA-containing, hypotonic buffer. These results suggest that a reduction in Na_o causes Ca_i to increase, as would be predicted from the presence of a Na-Ca exchanger in these cells. Further, dilution of the extracellular medium and consequent cell swelling also increase Ca_i independent of the reduction in Na_o. Because of the variability in Ca_i and the uncertainty as to the effects of ionic strength on the f_{max}, these results should be considered preliminary. [Supported by NIH grant AM 01090.]

37. Determination of Ionized Calcium Concentration in Isolated Smooth Muscle Cells Using Quin 2 D. A. WILLIAMS,* D. E. WOLF, and F. S. FAY, *Department of Physiology, University of Massachusetts Medical Center, Worcester, Massachusetts; Worcester Foundation for Experimental Biology, Shrewsbury, Massachusetts*

Cytosolic free calcium ions have an important regulatory role in the contractile function of muscle cells. However, there have been few reliable estimates of resting free calcium concentrations within muscle cells and, in particular, in smooth muscle cells. Therefore, we have used the fluorescent Ca^{++} indicator quin 2 to measure the cytosolic Ca^{++} concentration of suspensions of freshly isolated smooth muscle cells. Cell suspensions were prepared by enzymatic disaggregation of slices of toad (*Bufo marinus*) stomach muscularis. Aliquots were incubated with quin 2 (initial external concentration 10 μM) for 20 min or, alternatively, diluted 10-fold after the 20-min period and incubated for a further 60 min. The cells were then centrifuged at low speed (250 *g*) for 10 min to remove unloaded quin 2 and resuspended in amphibian Krebs Ringer (AKR) containing 1.8 mM Ca^{++}. At various stages, samples were removed and the contractile state of the cells was determined using the Coulter Counter technique (Singer and Fay, 1977, *Am. J. Physiol.*, 232:C138). Fluorescence was measured using a fluorescence spectrophotometer and calibrated to allow determination of the free internal calcium concentration using the method of Tsien et al. (1982, *J. Cell Biol.*, 94:325). A correlation between contractile states, fluorescence measurements, and hence Ca^{++} concentrations was therefore possible in the same cell suspensions. Resting $[Ca^{++}]_i$ averaged 88 ± 4 nM (n = 12) in cells loaded in normal Ca_o AKR under these conditions. Cells maintained in low Ca_o AKR (0.18 mM Ca^{++}) averaged only 55 ± 3 nM (n = 5). Coulter Counter analysis of the contractile states of these loaded cells suggested that the normal $[Ca^{++}]_i$ may be significantly buffered by quin 2, as the cell dimensions indicated a distribution of cells more relaxed than that of the control cells. Cell suspensions that were loaded with a much lower quin 2 concentration (1 μM initial) or for a shorter time, and whose cell size distributions were indistinguishable from control samples, averaged a significantly higher $[Ca^{++}]_i$: 122 ± 3 nM (n = 7). Quin 2 therefore provides a method for determining the internal free Ca^{++} concentration, which may contribute useful information regarding the

threshold calcium concentration for contraction of smooth muscle. However, the potential buffering effects of quin 2 loaded in the millimolar range should not be routinely neglected. [D.A.W. is an Australian National Heart Foundation Overseas Research Fellow. Supported by H114523 from the NIH and by a grant from the Muscular Dystrophy Association.]

38. Measurement of Cytosolic Free Calcium Concentration in Isolated Rat Ventricular Myocytes Using Quin 2 S.-S. SHEU,* V. K. SHARMA,* and S. P. BANERJEE,* *Department of Pharmacology, University of Rochester School of Medicine and Dentistry, Rochester, New York* (Sponsor: M. F. Schneider)

The cytosolic free calcium concentration, $[Ca^{2+}]_i$, was measured in isolated myocytes using the Ca^{2+}-selective fluorescent indicator quin 2. Isolated myocytes were prepared from the ventricles of adult male Sprague-Dawley rats by enzymatic dissociation. The isolated myocytes were loaded with 50 μM quin 2-AM for 1 h. Fluorescence was measured at an excitation wavelength of 339 nm and an emission wavelength of 490 nm, using an Aminco-Bowman spectrofluorometer. The fluorescence signal from resting cells indicated that $[Ca^{2+}]_i$ was 181 ± 18 nM (mean ± SEM, n = 18), which is very similar to the free cytosolic Ca^{2+} concentration measured by Ca^{2+}-sensitive microelectrodes (Sheu and Fozzard, 1982, *J. Gen. Physiol.*, 80:325). Inhibition of the Na-K pump with 0.1 mM strophanthidin produced an increase in $[Ca^{2+}]_i$, from 186 ± 17 to 736 ± 129 nM (n = 6). The results indicate that it is possible to measure $[Ca^{2+}]_i$ in cardiac myocytes that have been enzymatically isolated. Moreover, the results confirm the observation that inhibition of the Na-K pump can lead to an increase in $[Ca^{2+}]_i$, presumably via a Na-Ca exchange mechanism. [Supported by grant-in-aid 83:880 from the American Heart Association and by NIH grant AG03234.]

39. Fluorescence Emission Spectroscopy of 1,4-Dihydroxyphthallonitrile: a Method for Determining Intracellular pH in Cultured Cells IRA KURTZ* and ROBERT BALABAN, *National Heart, Lung, and Blood Institute, National Institutes of Health, Bethesda, Maryland*

We have characterized 1,4-dihydroxyphthallonitrile (1,4-DHPN) as a useful fluorescent probe for measuring intracellular pH (pH_i) in cultured cells growing in monolayers. This compound is unique since both its acid and base forms possess different fluorescence emission characteristics that can be used to quantitate pH_i. The fluorescence difference spectrum of an acid and alkaline solution of 1,4-DHPN has maxima at 455 nm, which corresponds to the acid form, and 512 nm, which corresponds to the base form. By determining the ratio of the intensity at these two wavelengths as a function of pH, a calibration curve was constructed. Since the two intensities are determined simultaneously, the measurement is independent of dye concentration, bleaching, and intensity fluctuations of the excitation source. Furthermore, analysis of the emission spectra permitted the detection of light scattering, binding effects, and chemical modification of the probe. A microspectrofluorometer was constructed to analyze low light level emission spectra from 1,4-DHPN within cultured cell monolayers. The instrument consists of a modified Leitz inverted microscope with a Ploem illuminator adapted for broadband excitation and objective focusing capabilities. The emission spectra were collected by impinging the fluorescence from the cell on a diffraction grating, which was scanned by a SIT camera interfaced with a computer. This permitted the acquisition of fluorescence emission spectra from 350–625 nm in ~33 ms. Initial studies have revealed evidence for pH_i regulation in the cultured epithelial cell line A6. The control pH_i was 7.49 ± 0.04 (n = 12) with the external pH at 7.6. Varying the external pH between 6.5 and 8.5 caused pH_i to change only 0.12 pH unit per unit change in the external medium. In addition, after acid loading the cells with ammonium chloride, pH_i returned to its original value with a time constant of ~6.5 min. The energy requirements of pH_i regulation in these cells are presently under investigation.

40. Na^+-H^+ Exchange in Gastric Glands as Measured with a Cytoplasmic-trapped, Fluorescent pH Indicator ANTHONY M. PARADISO,* ROGER Y. TSIEN, and TERRY E. MACHEN, *Department of Physiology-Anatomy, University of California, Berkeley, California*

We have used the pH-sensitive, fluorescent, cytoplasmic-trapped dye 2',7'-*bis*(carboxyethyl)-5,6-carboxyfluorescein (BCECF) in physiological experiments to identify Na^+-H^+ exchange in gastric glands isolated (high-pressure perfusion and collagenase digestion) from rabbit stomachs. The fluorescence of BCECF-loaded glands was calibrated in terms of cytosolic pH (pH_c) by permeabilizing the cell membranes and then titrating the extracellular solution to different pH values. In one set of experiments in Cl^--free solutions, glands were treated with 10^{-4} M ouabain for 45 min to increase cell $[Na^+]_c$ to high levels. Subsequent suspension of these cells in a Na^+-free Ringer's (to generate $[Na^+]_c > [Na^+]_o$) caused cells to acidify rapidly ($t_{1/2}$ = 60 s) from pH_c 7.15 down to pH_c 6.55. Subsequent addition of 100 mM Na^+ or Li^+, but not K^+, caused cells to realkalinize rapidly ($t_{1/2}$ = 30 s) toward control pH_c. The rate of realkinization did not appear to be affected by the presence of Cl^- in the media, but it was increased in hypertonic solutions. These changes of pH_c were blocked when ouabain-treated glands had been pre-equilibrated for 10 min with 1 mM amiloride, and this block was overcome by adding 10 μM monensin (an ionophore that artificially exchanges Na^+ for H^+). In another set of experiments in Cl^--Ringer's, glands were acid loaded by treatment with 30 mM NH_4Cl for 4 min followed by washing the NH_4Cl from the solutions. Under these conditions, pH_c decreased from 7.02 to 6.6; subsequent alkalinization of cells back to control pH_c was stimulated by Na^+ ($t_{1/2} \approx 1$ min), but not K^+, and was inhibited by 1 mM amiloride. This amiloride block was also overcome by further addition of 10 μM monensin. Rates of Na^+-dependent pH_c regulation were also increased in hypertonic solutions. We conclude that gastric glands contain a Na^+-H^+ exchanger that is independent of Cl^-, not activated by K^+, blocked by 1 mM amiloride, and accelerated by hypertonicity. This exchanger is likely localized to the serosal membrane of gland cells. Na^+-H^+ exchange may play an important role in regulation of pH_c in oxyntic and chief cells exposed to very high luminal acidity, where back-diffusion of H^+ into cells may occur at rapid rates. [Supported by NIH grants AM19520 and GM07379.]

41. K and Cl Conductance of Valinomycin-treated Human Red Blood Cells, as Determined with the Fluorescent Potentiometric Indicator WW781

JEFFREY C. FREEDMAN and TERRI S. NOVAK,* *Department of Physiology, State University of New York-Upstate Medical Center, Syracuse, New York*

Unbuffered suspensions of fresh, washed human red blood cells were incubated at 1.2% hematocrit for 30 min at 23°C in x mM KCl, 150 − x mM NaCl (x = 1–150 mM), and with or without 10 μM of the anion transport inhibitor DIDS. For each K_o (1–150 mM), 3.5 μM WW781 was added, and aliquots were transferred to cuvettes to measure the diffusion potentials (ΔE_m) induced by 1 μM valinomycin (VAL) (see Freedman and Novak, 1983, *J. Membr. Biol.*, 72:59). After adding 1 μM VAL to the remainder of each suspension, net effluxes of K and Cl were determined. The VAL-induced changes in WW781 fluorescence ($\%\Delta F_{VAL}$) were calibrated at each K_o by recording ΔpH_o upon subsequent addition of 1 μM proton ionophore FCCP. Assuming proton equilibrium for DIDS-treated cells, $\Delta E_m = -(2.303\ RT/F)\ \Delta pH_o$. Dye calibration was 0.15 ± 0.01 $\%\Delta F$/mV (SD, n = 3) between 0 and −110 mV, at least twice the linear range of diS-C_3(5). Proton fluxes after FCCP were insufficient to alter ΔE_m. DIDS increased both $\%\Delta F_{VAL}$ and ΔpH_o. If the dye calibration in DIDS-treated cells pertains to cells without DIDS, then the relation between E_m and K_o is well described by the constant field theory, such that DIDS increases $P_{K\cdot VAL}/P_{Cl}$ from 10 to 123. Without DIDS, computing ΔE_m directly from ΔpH_o overestimates ΔE_m by up to 20 mV, compared with values from WW781 fluorescence. From the net K and Cl fluxes and from the diffusion potentials at varied K_o, current-voltage plots were constructed (i_K and i_{Cl} vs. $E_m - E_K$ and $E_m - E_{Cl}$, respectively). In three experiments with cells from normal donors, K conductance, $g_{K\cdot VAL}$, was constant at 0.55 ± 0.24 S/g Hb (SD, n = 3) between 0 and +25 mV, began to decrease above +25 mV, and was unaffected by DIDS. By this analysis, Cl conductance, g_{Cl}, was constant at 0.39 ± 0.02 S/g Hb (SD, n = 3) between 0 and −60 mV and was 96 ± 4% inhibited (SD, n = 3) by DIDS. [Supported by NIH grant GM28839 and by the American Heart Association/Upstate New York Chapter, Inc.]

42. Use of the Cyanine Dye diS-C_3-(5) to Monitor Electrochemical Changes in Membranes During Assembly of the Terminal Complement Proteins C5b–9

T. WIEDMER* and P. J. SIMS,* *Department of Pathology, University of Virginia School of Medicine, Charlottesville, Virginia* (Sponsor: P. K. Lauf)

The cytolytic acitivity of the serum complement system resides in the capacity of the five terminal proteins—C5b, C6, C7, C8, and C9—to bind to membranes and increase their permeability to aqueous solute, thereby collapsing transmembrane electrochemical gradients. The equilibration of Na^+ and K^+ across the damaged plasma membrane is accompanied by the colloid-osmotic expansion of cell water, leading ultimately to cell death. Increasing evidence is accumulating that the C5b–9 proteins may also mediate sublytic alteration of membrane function of potential biomedical significance. The fluorescent cyanine dye diS-C_3-(5) has been used to monitor the membrane potential of red blood cells during complement-mediated hemolysis. Antibody-coated human erythrocytes treated with complement proteins C1–C7 and suspended in physiological NaCl (KCl) buffer were exposed to the K^+ ionophore valinomycin, resulting in hyperpolarization (or depolarization) of the cells. Subsequent sequential addition of the complement proteins C8 and C9 allowed real-time observation of the collapse of the valinomycin-induced membrane potential. Under conditions of limiting input of C8, collapse of the membrane potential occurred in the absence of a significant amount of hemolysis. Changes in membrane potential upon C5b–9 assembly could also be observed when red cells, equilibrated in SO_4^{2-} and subsequently exposed to the anion transport inhibitor DIDS, were used as target membranes. In conclusion, monitoring the membrane potential with the fluorescent probe diS-C_3-(5) is a fast, simple, and sensitive method to directly measure sublytic changes in membrane function. [Supported by a grant-in-aid from the American Heart Association and by the Jeffress Trust. P.J.S. is a John A. Hartford Fellow.]

43. Diffusion of Fluorescent Dyes in Segmented Axons PETER R. BRINK, STEWART W. JASLOVE,* and S. V. RAMANAN,* *Anatomical Science Health Science Center, School of Medicine, State University of New York, Stony Brook, New York*

We are using optical techniques to monitor the diffusion of fluorescent dyes within segmented axons from invertebrate nerve cords. These are cylindrical cells joined end to end by electrotonic synapses to form a functionally syncytial single giant axon. Our preparations are the medial axon of the earthworm (diameter 0.08 mm, segment length 1 mm) and the lateral axon of the crayfish (diameter 0.1 mm, length 5 mm). Microelectrodes are used to iontophoretically inject a fluorescent dye into a centrally located cell. Once the cell is filled, and before significant amounts of dye can diffuse across end-junctions into adjacent cells, the electrodes are removed and the nerve chamber is mounted on a noninverted, epi-illuminated fluorescent microscope, fitted with a motorized stage and a spot photomultiplier. Excitation and barrier wavelengths are set by a pair of grating monochrometers. The photomultiplier records from a 0.05-mm-diameter spot, which is automatically scanned along the axis of the axon at a rate of 0.1 mm/s. The photomultiplier output is sampled by an analog-to-digital convertor and transferred to a microcomputer for plotting and storing. On-line, high-speed storage is provided by a 15-Mb hard disk. Scans taken at intervals after injection provide a record of the time course of dye diffusion along the chain of cells. When fit to a computer model of axial diffusion in this system, the data allow unambiguous determination of apparent axoplasmic diffusion coefficients and junctional membrane permeabilities for different dyes. Various analogues of lucifer and fluorescein dyes are being studied. Preliminary data indicate that earthworm junctions are less permeant to dyes than crayfish junctions. The fluorescent intensity of the short earthworm segments (separated by transverse septa) differ by step functions, with the injected cell decreasing with time and adjacent cells increasing. The long crayfish axons (with oblique septa) show simple axoplasmic dye diffusion in the direction away from the septa, and a three-length constant intensity change (axon-overlap-axon) across the septa. [Supported by NIH grant GM 24905 to P.R.B.]

44. NBD-Taurine Fluorescence as a Probe of Anion Exchange in Intact Gallbladder Epithelium KEVIN FOSKETT,* *National Heart, Lung, and Blood Institute, National Institutes of Health, Bethesda, Maryland*

After osmotic shrinkage of *Necturus* gallbladder epithelial cells, the cells restore their volumes to control levels despite the continued presence of the hyperosmotic medium. Activation of parallel neutral Na-H and Cl-HCO_3 exchangers in the apical membrane appears to be necessary for volume regulatory increase. To determine whether ion flux through the anion exchanger is actually enhanced by exposure to hypertonicity, fluorescence measurements of NBD-taurine,

a substrate of the anion exchanger in red blood cells, have been made in intact *Necturus* gallbladder. The cells were loaded with the dye by incubation. The tissue was perfused in a miniature Ussing-type chamber placed on the stage of a microscope and viewed with high-magnification optics (100× oil immersion lens; 1.3 numerical aperture) combined with image-intensified video. Under computer command, a shutter was momentarily activated (open time = 680 ms) to allow the preparation to be excited by the 476-nm line of an argon ion laser by epi-illumination. The fluorescence was monitored with a photomultiplier tube; the transmittance of the tissue to the 476-nm laser excitation light was monitored with a photodiode. The epithelium was simultaneously observed by oblique illumination with transmitted 620-nm light to control for changes in focus or lateral movement. Fluorescence intensity, corrected for lens and tissue autofluorescence and for bleaching, decayed over time as NBD-taurine left the cells and was washed away by the rapid solution flow through the chamber. Exposure of the tissue to a mucosal medium made hypertonic by the addition of mannitol enhanced the efflux of NBD-taurine from the cells in ~70% of the tissues examined. In the presence of the anion exchange inhibitor SITS (100 μM), hypertonicity enhanced NBD-taurine efflux in only 14% of the preparations. Hypertonicity also caused changes in tissue optical transmittance, but these could not be correlated with changes in NBD-taurine fluorescence. The data support the previous contention that hypertonicity activates a SITS-sensitive Cl-HCO_3 exchange process in these cells.

45. Image-intensified Recording of Co-Localized Bioluminescent Flashes and Fluorescence from Subcellular Organelles in the Dinoflagellate *Gonyaulax* CARL H. JOHNSON, J. W. HASTINGS, and SHINYA INOUÉ, *Harvard University Biological Laboratories, Cambridge, Massachusetts; Marine Biological Laboratory, Woods Hole, Massachusetts*

Using an inverted microscope coupled to a Zeiss/Venus three-stage intensified camera, we have determined that the bioluminescent flashes of the marine dinoflagellate alga *Gonyaulax polyedra* originate from many discrete subcellular loci which co-localize with autofluorescent granules (~0.5 μm in diameter). Dozens of these fluorescent granules are located in the cortex of each cell. This endogenous fluorescence is similar in color to bioluminescence and is lost after exhaustive stimulation of bioluminescence. These facts suggest that the fluorescence is attributable to the bioluminescent substrate luciferin; additional support for this idea derives from experiments in which the fluorescence and bioluminescence of granules in vitro is restored by the addition of purified luciferin. The fluorescence in vivo, as measured by flow cytometry (in collaboration with Dr. Sam Latt, Children's Hospital, Boston, MA), exhibits classical circadian properties: under constant conditions (dim light), the intensity of the granules is rhythmic (while the number of granules per cell appears to be constant). The in vivo fluorescence is maximal in the middle of the night phase and is low during the day. Thus, luciferin seems to be localized within the cell to discrete organelles from which the bioluminescence emanates; the cellular quantity of luciferin is rhythmically modulated by the circadian clock. [Supported by grants from the NSF and NIH.]

46. Optical Recording of Calcium Responses from Nerve Terminals of Frog Neurohypophysis A. L. OBAID, R. K. ORKAND, H. GAINER, and B. M. SALZBERG, *Department of Physiology and Pharmacology, University of Pennsylvania School of Dental Medicine, Philadelphia, Pennsylvania; Laboratory of Neurochemistry and Neuroimmunology, National Institutes of Health, Bethesda, Maryland*

Voltage-sensitive dyes were used to record membrane potential changes by optical means from nerve terminals in the isolated frog neurohypophysis. Following the block of voltage-sensitive Na^+ channels by tetrodotoxin (TTX) and K^+ channels by tetraethylammonium (TEA), direct electric field stimulation of the nerve terminals still evoked large active responses. These responses were reversibly blocked by the addition of 0.5 mM cadmium chloride. At both normal and low $[Na^+]_o$, the regenerative response appeared to increase with increasing $[Ca^{2+}]_o$ (0.1–10 mM). There was a marked decrease in the response at low $[Ca^{2+}]_o$ when $[Na^+]_o$ was reduced from 120 to 8 mM (replaced by sucrose), but little if any effect of this reduction of $[Na^+]_o$ at normal $[Ca^{2+}]_o$. These local responses most probably arise from an inward Ca^{2+} current

associated with hormone release from these nerve terminals. At low $[Ca^{2+}]_o$, Na^+ appears to contribute to the TTX-insensitive inward current. [Supported by USPHS grants NS-16824 and NS-12253.]

47. Topological Spectral Scanning of Single Cells R. S. BALABAN, I. KURTZ,* H. CASCIO,* and P. SMITH,* *National Heart, Lung, and Blood Institute, and Division of Research Services, National Institutes of Health, Bethesda, Maryland*

A technique is described which permits the simultaneous acquisition of multiple fluorescent emission and/or absorption spectra from discrete regions of a single cell. The instrument consists of a modified Leitz microscope, optical grating, SIT camera, and digital video image processor. An optical slice of the cell is selected by positioning the entrance slit of the grating over the region of interest, while observing the zero-order diffraction of the grating with the SIT camera. In order to obtain the spectral characteristics of this optical slice, the grating is rotated to impinge the first-order diffraction on the SIT. The video image of the first-order diffraction is an optical spectrum of the slit. Since this video image of the first-order diffraction maintains its orientation in the long axis of the slit, each horizontal line (or track) of the video image contains the spectral characteristics of the corresponding vertical position in the slit with a resolution of 1/500th of the spectral window of the grating. Therefore, this "spectral image" collected by the camera consists of 500 individual spectra, all from discrete regions along the slit. The image-processing system acquires and processes all 500 spectra in ~1 s and permits the accurate localization of the source of each spectrum in the cell image. Scanning of the entire cell, instead of a single slice, is possible by systematically moving the slit or microscope stage and acquiring spectral images throughout the cell. This method permits the rapid simultaneous acquisition of optical spectra from discrete regions of the cell. The topological spectral analysis permits the detection of and possible correction for photobleaching, light scattering, and image plane effects. In addition, environmental and metabolic modifications of the spectral characteristics of intracellular chromophores can be detected. The use of this spectral imaging technique will be demonstrated on cultured epithelia and living rabbit blastocysts monitoring both intrinsic and extrinsic chromophores.

48. Regional Properties of Neurons Studied with Voltage-sensitive Dyes and Calcium Indicator Dyes W. N. ROSS,* N. STOCKBRIDGE,* L. LEWENSTEIN,* and V. KRAUTHHAMER,* *Department of Physiology, New York Medical College, Valhalla, New York* (Sponsor: L. B. Cohen)

Regional potential changes and calcium influx were monitored in neurons of the giant barnacle, ***Balanus nubilus***, using a 10 × 10 array of photodiodes. These recordings were correlated with specific positions on the cell by injecting them with the fluorescent dye Lucifer Yellow. Supraesophageal ganglia were mounted on the stage of a compound microscope and imaged onto the photodiode array with each element corresponding to 40 × 40 μm^2 in the object plane. For voltage measurements, the preparation was stained with the probe NK2367 and illuminated with constant intensity light at 720 ± 15 nm. The soma was repetitively stimulated with depolarizing and hyperpolarizing pulses and the changes in light intensity detected by the photodiode elements were averaged. Clear signals were detected from most positions on the cells, including fine processes. Controls established that the signals corresponded to voltage changes at each position and that they originated only from the stimulated cell. Using this approach, we examined the site of action potential initiation and the propagation of active and passive potentials within the cell. In some cells, active dendrites were demonstrated. For calcium experiments, the dye arsenazo III was iontophoresed into the soma and allowed to diffuse throughout the cell. When the cell was stimulated, absorption changes at 640 ± 30 nm were recorded at each position. Spectral measurements and blockage by external cobalt established that the signals resulted from calcium entering from the external medium. Since calcium diffuses slowly in axoplasm, changes at each position indicate the location of calcium channels in the membrane. For many neurons, calcium channels were found on the soma, axon, and dendritic processes. In the photoreceptor, calcium channels were concentrated in the presynaptic terminal. A comparison of the time course of the signals at different positions suggests that calcium entry saturates faster in the processes than in the soma or axon. [Supported in part by USPHS grant NS16295, NRSA Fellowships NS07172 and NS06929, and the Irma T. Hirschl Foundation.]

49. Multiple-Site Optical Recordings of Action Potentials (APs) and NADH Fluorescence from "Working" Mammalian Heart Preparations GUY SALAMA and RICHARD LOMBARDI, *Department of Physiology, University of Pittsburgh School of Medicine, Pittsburgh, Pennsylvania*

Mammalian hearts were cannulated at the aorta and left ventricle, perfused in a "working" heart apparatus, and stained with a voltage-sensitive merocyanine dye. In some experiments, the right atrial and ventricular walls were surgically removed to expose the interventricular septum and the specialized pathways for electrical conduction. Krebs-Henseleit solutions were gassed with 95% O_2/5% CO_2 or with 95% N_2/5% CO_2 to induce anoxias. Light from tungsten-halogen lamps was collimated and passed through appropriate interference filters, and illuminated the heart uniformly. Fluorescent or reflected light was collected to form an image of the whole heart, or a selected region of the myocardium, on a 12 × 12 photodiode array by varying the magnification of the image. The heart was placed in a chamber and pushed against a glass window to reduce its natural curvature and its motion during contractions. Signals from 124 elements of the array were amplified, either AC-coupled with a 3-s time constant to preserve the shape of APs, or DC-coupled to measure intrinsic NADH fluorescence, and then stored for analysis. Signals from each diode were sampled every 0.6 s for 2–4 s. A series of linear regressions was performed on each optical trace to locate AP upstrokes, determine delays between APs from various regions of the heart, and draw maps of propagation pathways. A scan was analyzed in <20 s. Changes in AP duration and patterns of propagation were correlated with the local metabolic state of the tissue through its NADH fluorescence. Ca^+ entry blockers, β-adrenergic antagonists, nitrogen anoxias, and local ischemias induced by ligating a coronary vessel were found to produce characteristic changes in the normal patterns of electrical propagation. [The authors thank Dr. Lawrence Cohen for his valuable advice. Supported by AHA grant 82 1231 and by the Western Pennsylvania Affiliate of the AHA.]

50. Computer-based Determination of Epithelial Cell Size and Shape DONALD J. MARSH, PETER KOCH JENSEN, and KENNETH SPRING, *Laboratory of Kidney and Electrolyte Metabolism, National Institutes of Health, Bethesda, Maryland*

Measurement of cell volume in living epithelial cells has become an important technique in studies of membrane transport processes that function in cell volume regulation. The cross-sectional area of optical sections of the epithelial cells is determined by planimetry of video images. The cell volume is calculated from the measured area of each section and the known focus displacements. In the past, the measurement of cross-sectional area has been done by manual positioning of a cursor superimposed on the video image. Each experiment generates ~200 images in which two or more cells may be analyzed We have developed a computer-based method that uses one image as a template and allows automated area determination of successive images by template matching and digital image processing. This new method is comparable to the older method in speed and accuracy, but it requires much less effort from the experimenter. The images are first stored on a video disc recorder and subsequently analyzed off-line by an image processor connected to a computer. The investigator generates an outline of the first image of the epithelial cell, and the computer uses this outline as a template for edge detection in the other images. Template matching is achieved by a combination of digital filtering, covariance, and shape-matching techniques. The first cell image is used as a template for each successive image in a stack of slices taken at one time; the detected edges are then used to form templates for each focal plane at successive times.

51. Measurement of Cell Membrane Water Permeability in Rabbit Cortical Collecting Tubule K. STRANGE* and K. R. SPRING, *National Heart, Lung, and Blood Institute, National Institutes of Health, Bethesda, Maryland*

We have recently developed the method logy to measure directly apical and basolateral membrane water permeability (L_p) in cells of the mammalian cortical collecting tubule (CCT). Rabbit CCT are dissected and perfused in vitro at 37°C on the stage of a Nikon Diaphot inverted microscope equipped with Nomarski optics. CCT are viewed on a video monitor using a 63× oil immersion objective and a 32× objective-condenser lens with a 7-mm working distance. Cell borders and both tubule cell types (principal and intercalated cells) are easily

discernible using this optical arrangement. Membrane L_p is measured as the initial rate of cell volume change induced by a rapid change in serosal or mucosal osmolality. Rapid bath solution changes are made using a specially designed laminar flow chamber (95% washout in <1 s) and luminal solution changes are made using a continuously flowing fluid exchanger pipette or a double-barreled perfusion pipette arrangement. The cell volume is determined using a combination of optical cell-sectioning techniques and measurement of the cross-sectional area of cells in the tubule wall. We are currently examining the role played by antidiuretic hormone in regulating apical and basolateral membrane water permeability in both principal and intercalated cells.

52. Segmentation of Three-Dimensional Cell Images for Graphic Modeling and Analysis JAMES M. COGGINS, FREDRIC S. FAY, and KEVIN E. FOGARTY, *Computer Science Department, Worcester Polytechnic Institute, and Department of Physiology, University of Massachusetts Medical Center, Worcester, Massachusetts*

Computer analysis of cell images often requires the location of structures of interest within an image and the measurement of salient features of those structures for use either in developing graphic display models or in automatic decision-making. Ongoing studies of the mechanism of force generation in single smooth muscle cells require a graphic model for depicting the locations and orientations (in three dimensions) of elongated bodies rich in the protein α-actinin. These bodies are believed to be integral parts of the contractile mechanism whose organization we wish to understand. In relaxed cells, these bodies are on the average 1.25 μm long and 0.25 μm wide, and are oriented within 15° of the cells' long axis. To assess the pattern of organization of these bodies, we obtain a set of optical sections of the pattern of fluorescence caused by fluorescently labeled anti-α-actinin in a single cell. An iterative deconvolution procedure is applied to the three-dimensional (3D) data set to reduce distortion caused by the image acquisition system. Subsequent analysis to determine the position and orientation of all α-actinin–rich bodies is performed by an artificial visual system consisting of three 3D spatial filter sets. In the first stage of analysis, local maxima in the output of one filter are thresholded to locate body centers. Next, the pattern of responses of each body to a set of four filters is used to determine the angle θ between the long axis of the body and the long axis of the cell. A set of six filters is used to determine the orientation ϕ of the projection of the long axis of the body on a plane normal to the long axis of the cell. The resulting information about the 3D position and orientation of all α-actinin–rich bodies in a cell is used to analyze the organization of the contractile apparatus in smooth muscle. The use of this artificial 3D visual system in analyzing other aspects of cellular organization is presently being explored. [Supported in part by NIH grant HL14523 and by the Muscular Dystrophy Association.]

53. Asymmetric Illumination Contrast: a Method of Image Formation for Video Light Microscopy BECHARA KACHAR,* *Laboratory of Neurobiology, National Institutes of Health, Bethesda, Maryland* (Sponsor: K. R. Spring)

Images with high resolution and an exceptionally broad gray scale can be obtained by the application of video contrast enhancement to an optimized procedure for imaging transparent objects with oblique rays of illumination. When a bright field microscope is operated conventionally at high numerical aperture and in Kohler illumination, the most oblique rays of the illuminating beam produce diffracted light which spreads out from each detail of the object such that up to one-half of each cone of diffracted light (i.e., a side band) is outside of, and thus excluded from, the objective aperture. The portion of such diffracted light that enters the objective would by itself be able to form an amplitude-modulated image by interference with the respective direct light (Ellis, 1978, *In* Cell Reproduction), but no image of the transparent object is produced because opposing rays of the symmetric illuminating cone produce complementary interference patterns that consequently cancel each other. This balance is offset by making the illumination asymmetric. A visible image results from the difference of intensity between interference patterns of the diffracted light from opposing oblique rays of the illuminating cone. However, the contrast of the image seen directly in the microscope is very low because of the large amount of light scattered from regions of the specimen not in the field of view. Image contrast can be amplified electronically by connecting a TV camera to the microscope (Inoue, 1981, *J. Cell Biol.*, 89:346). Features such as high resolution, optical

sectioning, control of contrast, and operation under low light intensity make this technique preferable, in several instances, to currently used video microscopy techniques, particularly for viewing thick living specimens. These advantages increase the versatility and range of application of video-enhanced light microscopy to virtually any type of specimen.

54. Reflection Spectrometry on Innervated Brown Fat: Validation of the Method and Application to a Study of the Correlation Between α- and β-Adrenergic–mediated Changes of Membrane Potential and Metabolism G. SCHNEIDER-PICARD, J. P. GIACOBINO, and L. GIRARDIER, *Department of Physiology and Department of Medical Biochemistry, University of Geneva Medical School, Geneva, Switzerland*

A reflection spectrometer was developed that allows simultaneous and continuous measurement of reflected light intensity at specific absorption and fluorescence wavelengths. From the spectral characteristics of the reflected light or emitted fluorescence, and from the effects of substrates and a metabolic inhibitor on their intensities, it was shown on a brown fat in vitro preparation that the absorption and fluorescence signals at an excitation wavelength of 465 nm are associated with different flavoproteins. The fluorescence signal appears to be due mainly to changes in the redox state of flavoproteins beyond site I, and the absorption signal to changes in the redox state of flavoproteins in the fatty acid β-oxidation pathway (acyl-CoA dehydrogenase step). An endocrine disorder, streptozotocin diabetes, was used to correlate the specific activities of the enzymes of β-oxidation in brown fat homogenates, determined biochemically, to spectrometrically determined specific activity of β-oxidation on whole tissue preparations from the same animals. Taken together, the results suggest that changes recorded with the reflection spectrometer in response to electrical nerve stimulation, exogenous noradrenaline, and substrate addition are due essentially to changes in the metabolic activity of the tissue. Membrane potential and flavoprotein redox states were measured simultaneously and continously in order to determine the temporal relationship between membrane potential changes and metabolic activity in response to tissue stimulation. A first rapid depolarization, which was almost completely blocked by an α antagonist, precedes the increase in flavoprotein oxidation or reduction. A second slow depolarization follows the maximum changes in flavoprotein redox states. A β antagonist delays the first repolarization until the end of stimulation and inhibits transient hyperpolarization, second depolarization, and flavoprotein reduction. Thus, brown fat contains both α- and β-adrenergic receptors mediating different electrical and metabolic events in response to tissue activation. [Supported by grant 3.071.081 from the Swiss National Science Foundation.]

55. Photodynamic Action of Halogenated Fluorescein Derivatives on Smooth Muscle Cells E. K. MATTHEWS and D. E. MESLER, *Department of Pharmacology, University of Cambridge, Cambridge, England*

Photon activation of tetraiodofluorescein (erythrosine) elicited a marked contraction of the smooth muscle cells of the guinea pig taenia coli superfused in vitro. Neither high-intensity illumination alone (up to 5×10^4 lx) nor erythrosine alone (up to 2×10^{-4} M) affected the tone of the taenia preparation or its ability to respond to a test agonist (carbachol). Photoirradiation of erythrosine before tissue contact was also ineffective. The magnitude of the photodynamic contraction was dependent upon the concentration of erythrosine (2×10^{-9}–2×10^{-4} M), the intensity (2×10^3–5×10^4 lx) and wavelength of the incident light (action spectrum peak 538 nm), and the presence of oxygen and Ca^{2+}. The effect was blocked by N_2, dithionite (1 mM), or EGTA (1 mM). Tetrachlorotetraiodofluorescein (Rose Bengal) was more potent and tetrabromofluorescein (eosin) less potent than erythrosine. These results are consistent with a photochemical "skinning" or "membrane stripping" action in which the dye-dependent generation of highly reactive singlet-excited oxygen increases plasma membrane permeability to Ca^{2+} by local peroxidation of membrane proteolipid and so initiates muscle contraction. This technique for the photodynamic modulation of membrane calcium permeability is applicable not only to smooth muscle cells; it can be extended also to secretory, epithelial, and myocardial cells.

56. Voltage Dependence of Acetylcholine Receptor Channel Opening in Rat Myoballs LEE D. CHABALA* and HENRY A. LESTER, *Division of Biology, California Institute of Technology, Pasadena, California*

Previous studies, largely restricted to hyperpolarized membrane potentials, have shown that the effective opening rate (β') of the acetylcholine (ACh) receptor channel has only a shallow voltage dependence. We sought to study this voltage dependence in more detail by extending the measurements to positive potentials. Whole cell currents from ACh channels were recorded from voltage clamped rat myoballs. Most of the Na^+ and K^+ channels were inactivated by holding the membrane potential near 0 mV: the residual outward K^+ currents were suppressed by using either NaCl or CsCl in the recording pipette. The myoballs were bathed in a solution containing 500 nM pure *cis-Bis*-Q (the inactive isomer), and a light flash was used to produce an agonist concentration jump from 0 to >270 nM *trans-Bis*-Q (i.e., at least 100 times lower than the half-maximal concentration) at various voltages between −160 and +110 mV. The kinetic and steady state properties of the resulting macroscopic current relaxations were studied. Once the steady state conductance is normalized for the (measured) open channel conductance at each voltage, it shows an (approximately) exponential increase with hyperpolarization. The apparent channel closing rate (α ~0.07 ms^{-1} at −100 mV, 15°C) decreases with hyperpolarization but cannot account for the observed voltage dependence of the conductance. In addition, α saturates at positive potentials. β' shows the opposite voltage dependence: it decreases strongly with membrane potential at positive voltages and tends to saturate at hyperpolarized membrane potentials. Because the total number of channels in a myoball cannot be estimated with precision, β' was determined to within a multiplicative constant (i.e., its voltage dependence, but not amplitude, was measured). The tendency for the transition rates to saturate at high field strength can be understood if each rate constant depends differently on both the first and second power of membrane potential (Stevens, 1978, *Biophys. J.*, 22:295). Thus, the membrane dielectric shows both orientation and distortion polarization. Typical values (assuming a membrane thickness of 50 Å) for the effective dipole moment component are ~31 Debye for α and ~47 Debye for β', while typical distortion polarizability components are ~(38 Å)^3 for α and ~(45 Å)^3 for β'. [Supported by USPHS grant NS-11756 and by a fellowship from the Muscular Dystrophy Association to L.D.C.]

57. Fluorescent Macroscope: an Instrument to Screen for Clones of Attached Cultured Cells Having Different Fluorescent Properties ROBERT J. DINERSTEIN* and MITCHEL L. VILLEREAL, *Department of Pharmacological and Physiological Science, University of Chicago, Chicago, Illinois*

In recent studies with cultured human fibroblasts, we have used a sensitive computerized microspectrofluorometer (1) and specific intracellular fluorescent probes to demonstrate a rise in intracellular pH and Ca activity in response to mitogen stimulation (2, 3). Since it would be valuable to select mutants of fibroblasts that have altered pH and Ca responses to mitogen stimulation, we investigated methods for screening a large number of fibroblasts for variations in intensity of probe fluorescence. Therefore, we developed an optical system, which we call the fluorescent macroscope, which can screen an entire 100-mm culture dish. The time course of mitogen-induced changes in cellular fluorescence of up to 10^4 fibroblast colonies, each presumably arising from a single cell, can be compared simultaneously. Thus, non-responders or over-responders can be identified and later selected with a cloning ring. We have to date been successful in visualizing and photographing dishes containing colonies of cultured mouse fibroblasts (3T3 cells) loaded with the pH dye dimethylcarboxyfluorescein. When the cells are exposed to NH_4Cl to alkalinize the cells, one can discern a rise in fluorescence of the macroscopic colonies. Since each dish can be rapidly screened, one could easily screen 10^6 cells in a matter of hours. Thus, using this instrument in conjunction with pH indicators provides an opportunity to screen large numbers of attached cells for variability of their pH response to stimuli. Similar screens based on other fluorescent indicators (e.g., for Ca) also should be feasible. [Supported by NIH grants GM 28359, GM 22220, and DA 02575 and NIH RCDA AM 01182 (M.L.V.).]

1. Dinerstein, R. J., et al. 1979. *Science (Wash. DC)*. 205:497.
2. Mix, L. L., R. J. Dinerstein, and M. L. Villereal. 1984. *Biochem. Biophys. Res. Commun.* 119:69.
3. Mix, L. L., R. J. Dinerstein, and M. L. Villereal. 1984. *Biophys. J.* 45:86*a*. (Abstr.)

58. Evidence for a Series Barrier to Ion Transport in Rabbit Distal Colon STEPHEN M. THOMPSON, *University of Texas Medical School, Houston, Texas*

Segments of stripped rabbit distal colon were mounted in standard Ussing chambers and bathed on the mucosal side by a Na-gluconate Ringer and on the serosal side with a 100 mM K^+-gluconate Ringer in order to depolarize the basolateral membrane (BLM). Electronic compensation for the resistance of the fluid between the voltage-sensing electrodes was made before mounting the tissue in the chamber. Transepithelial current-voltage relations were measured before and after addition of 10^{-4} M amiloride to the mucosal bath. The data were analyzed using an electrical equivalent circuit model, which includes a submucosal resistance, R^{sub}, in series with the cellular and paracellular pathways in order to derive the *I-V* relation for Na entry across the apical membrane. For this analysis, it was assumed that K^+ eliminated the resistance and emf of the BLM so that the transapical membrane voltage is given by $\psi^{mc} = \psi^{ms} + I^{ms}R^{sub}$. For $R^{sub} = 0$, these *I-V* relations were nonlinear, but consistently deviated from the predictions of the GHK flux equation. In each case, however, a good fit by the flux equation could be obtained by assuming a nonzero value for R^{sub} (23.4 ± 2.0 Ωcm^2, $n = 40$). Subsequently, a detergent (0.3% Lubrol) was added to the mucosal bath, causing a marked decrease in tissue resistance to 20.2 ± 3.3 Ωcm^2, $n = 10$. The tissues were then fixed and examined using light and electron microscopy (courtesy of Dr. K. Karnakv and L. Garretson), which showed that the detergent had denuded the epithelium of surface cells, but had left the crypts and basal laminae intact. The agreement between the resistance of the denuded epithelium and the value of R^{sub} required to make the *I-V* relation for Na entry fit the GHK flux relation suggests the existence of a subepithelial barrier to ion transport in intact tissues and may have major importance for the interpretation of electrophysiological data. [Supported by NIH grant GM31191.]

59. Electrogenic Anion Transport in Rabbit Distal Colon

J. H. SELLIN and S. M. THOMPSON, *Departments of Medicine and Physiology, University of Texas Medical School at Houston, Houston, Texas*

Basal anion transport in rabbit distal colon is thought to occur by electroneutral Cl:HCO_3 exchange, whereas Cl secretion stimulated by cAMP- and Ca-mediated agonists is an electrogenic process. Here we report effects of serosal SITS (0.5 mM) and furosemide (1 mM) on basal anion transport in amiloride-treated colonic segments mounted in Ussing chambers. Effects of SITS on I_{sc} ($\mu eq/cm^2 \cdot h$), tissue conductance (mS/cm^2), and Cl fluxes ($\mu eq/cm^2 \cdot h$) are given below for control tissues and tissues treated with amphotericin to functionally eliminate the apical membrane.

	I_{sc}	g_t	J^{Cl}_{ms}	J^{Cl}_{sm}	J^{Cl}_{net}
Control	−0.14	3.90	3.8	3.3	0.5
+ SITS	0.93*	2.94*	2.2*	2.2‡	0.1
Amphotericin	0.87	4.00	1.7	1.8	−0.1
+ SITS	2.49*	4.38	1.0‡	2.0	−1.0*

* $P < 0.01$; ‡$P < 0.5$.

In controls, removal of both Cl^- and HCO_3^- from the media abolished the effect of SITS on I_{sc}, but with either Cl^- or HCO_3^- present, SITS increased I_{sc}. Under control conditions, furosemide also increased I_{sc} (0.01 to 0.35, $P < 0.05$) while decreasing g_t and both J^{Cl}_{ms} and J^{Cl}_{sm}, but effects on J^{Cl}_{net} were not significant. In contrast, after amphotericin, furosemide decreased I_{sc} (2.53 to 1.76, $P < 0.05$), did not affect g_t, and decreased both J^{Cl}_{ms} (1.6 to 1.2, $P < 0.01$) and J^{Cl}_{sm} (2.2 to 1.0, $P < 0.01$), resulting in a significant increase in J^{Cl}_{net} (−0.6 to 0.2, $P < 0.05$). In K^+-depolarized epithelia, I_{sc} was increased by both SITS (−0.55 to −0.16) and furosemide (−0.48 to −0.18). Pretreatment with ouabain abolished the effects of both agents of I_{sc}. These results suggest a complex system for anion transport in rabbit distal colon such that, under appropriate conditions: (*a*) SITS decreases net Cl absorption, with this decrease accounting for half the observed increase in I_{sc}; (*b*) furosemide increased net Cl absorption, accounting for the entire change in I_{sc}. The mechanism(s) underlying basal electrogenic anion transport remains to be elucidated. [Supported by NIH grants AM01115 and GM31191.]

60. SITS Effects on the Proximal Tubule of the Rabbit Kidney Perfused In Vitro

BRUCE A. BIAGI,* *Department of Physiology, The Ohio State University, Columbus, Ohio*
(Sponsor: Jack A. Rall)

Conventional microelectrodes were used to study the effects of SITS (0.1 mM) in the bath on the intracellular potential, V_{bl}, of the superficial proximal straight tubule of the rabbit kidney perfused in vitro. Isolated tubules were luminally perfused with a solution resembling late proximal tubular fluid while the bathing solution contained a control solution resembling glomerular filtrate. The change in V_{bl} was measured when bath potassium concentration was increased (5 to 16.7 mM), bicarbonate was lowered at constant pH (22 to 6.6 mM), and sodium was lowered (146 to 0) in the absence and presence of SITS. Substituting ions were Na, Cl, and *N*-methyl-D-glucamine, respectively. A total of 72 cells were sampled from 14 tubules. The means ± SE (number of cells) were:

	Control	SITS
	mV	*mV*
V_{bl}	−44.6±2.05 (36)	−76.1±1.84 (45)
High K	+9.0±1.55 (29)	+24.4±0.81 (36)
Low HCO_3 (spike)	+16.0±4.24 (2)	+0.8±0.82 (7)
Zero Na	+33.3±2.27 (13)	+3.6±1.88 (8)

The new steady state V_{bl} was reached ~15 min after SITS exposure and was associated with marked cell swelling. The effects were not reversible following 1 h control perfusion. These results are consistent with the presence of a coupled sodium-bicarbonate carrier in the basolateral membrane, which is electrogenic and SITS inhibitable as described in the amphibian proximal tubule. SITS inhibition also results in an increase in potassium selectivity and cell swelling. [Supported by USPHS grant AM 30694.]

61. Cell Potassium Activity In Frog Skin Epithelium: Response to Voltage Clamping and Inhibition of Sodium Transport L. M. BAXENDALE,* J. F. GARCIA-DIAZ, and A. ESSIG, *Department of Physiology, Boston University School of Medicine, Boston, Massachusetts*

Cell K activity (a_K^c) was measured in the short-circuited frog skin (*Rana pipiens pipiens*) by simultaneous impalements from the apical surface with open-tip (1.5 M KCl, 40–80 Ω in Ringer's) and K-selective (Corning 477315 resin) microelectrodes. Short-circuit current (I_{sc}), apical membrane potential (V_o), the potential recorded with the K-selective microelectrode (V_K or $V_K - V_o$), fractional resistance of the apical membrane (F_o), total transepithelial conductance (g_t), and open-tip microelectrode resistance (R_{el}) were continuously displayed on a six-channel recorder. Strict criteria for acceptance of simultaneous impalements included constancy of R_{el}, agreement within 3% of F_o measured (400-ms pulses) with open-tip and K-selective microelectrodes, and constancy of $V_K - V_o$ for 30–60 s after application of amiloride or upon voltage clamping in the presence of amiloride. Skins were bathed on the serosal surface with NaCl Ringer's and, to reduce paracellular Cl conductance and effects of amiloride on paracellular conductance, with $NaNO_3$ Ringer's on the apical surface. Under control conditions, a_K^c was nearly constant among skins (mean ± SD = 93 ± 10 mM, 15 skins) in spite of a wide range of I_{sc} (5–70 $\mu A/cm^2$). Inhibition of Na transport with amiloride (20 μM) hardly affected a_K^c (97 ± 12 mM, $P > 0.4$), even 30 min after its application. V_o, which in control state ranged from −42 to −77 mV, hyperpolarized in amiloride, initially to −109 ± 5 mV, reaching a stable value after 16–26 min of −88 ± 5 mV. Thus, K was still above equilibrium (E_K = 99 + 3 mV, $P < 0.05$ for the difference $-V_o - E_K$) 30 min after inhibition of transepithelial Na transport. In nine experiments, removal of apical Na (*N*-methyl-D-glucamine or tetramethylammonium substitution) produced the same effects: a_K^c changed to 101 ± 9 mM ($P > 0.2$) and V_o hyperpolarized initially to −109 ± 9 mV. Clamping the transepithelial potential to values between −40 and +100 mV (apical reference) for 40–60 s did not produce any consistent effect on a_K^c in spite of significant and consistent effects on V_o, F_o, and cellular current. Application of serosal ouabain during short-circuit conditions induced a rapid depolarization of V_o (20 ± 10 mV) in the first 3 min; V_o then remained almost constant for ~30 min. a_K^c decreased continuously after 2 min in parallel with the decrease in I_{sc}. In the first 5 min, a_K^c decreased by 7–11% (0.1 mM ouabain) or 30–40% (1 mM ouabain); after 40 min, a_K^c was ~30 mM. [Supported by USPHS grant AM 29968 and (L.M.B.) USPHS Training Grant T32 AM07053.]

62. Basolateral Potassium Channel Block and Interactions Between the Cell Membranes of *Necturus* Urinary Bladder J. R. DEMAREST* and A. L. FINN, *Departments of Medicine and Physiology, University of North Carolina, Chapel Hill, North Carolina*

Experimental modulation of the apical membrane (AM) Na^+ conductance or the basolateral membrane (BM) Na^+-K^+ pump activity has been shown to result in parallel changes in BM K^+ conductance in a number of epithelia. To determine if modulation of BM K^+ conductance would result in parallel changes in AM Na^+ conductance and BM pump activity, *Necturus* urinary bladders stripped of serosal muscle and connective tissue were impaled through their BMs with microelectrodes in experiments that allowed rapid serosal solution changes. The apparent transference numbers (T_i) of the BM under control conditions for K^+ and Cl^- were determined from the effect on the BM electromotive force of a sudden increase in serosal K^+ from 2.5 to 50 mM/liter or a decrease in Cl^- from 101 to 10 mM/liter. T_K and T_{Cl} were 0.71 ± 0.05 and 0.04 ± 0.01; BM, therefore, is predominantly K^+ selective but has a small Cl^- conductance. Increasing serosal K^+ caused a marked reduction in the BM resistance (R_b), while decreasing Cl^- resulted in an increase in R_b. The K^+ channel blockers Ba^{+2} (0.5 mM) and Cs^+ (10 mM) reduced T_K to 0.52 ± 0.03 and 0.50 ± 0.07, while the commonly used K^+ substitute Rb^+ caused a smaller reduction of T_K. All three agents increased R_b by >75%. In each case, the increase in R_b was accompanied simultaneously by a significant increase in R_a of >20% and a decrease in transepithelial Na^+ transport. The increases in R_a, which were measured as a slope resistance, cannot be attributed to nonlinearity of the *I-V* relationship of the AM, since the changes in the measured cell membrane potentials caused by the K^+ channel blockers were not significantly different from those resulting from increasing K^+, which did not affect R_a. Thus, blocking BM K^+ conductance causes a reduction in net Na^+ transport by reducing K^+ exit from the cell and simultaneously reducing Na^+ entry into the cell across the AM. These interactions between components of the transepithelial Na^+ transport system are part of a network of feedback relationships that serve to maintain cellular homeostasis. [Supported by NIH grant AM17854.]

63. The Effect of Calcium Channel Blockers on the Electrophysiology of Guinea Pig Gallbladder PAMELA J. GUNTER-SMITH,* *Physiology Department, Armed Forces Radiobiology Research Institute, Bethesda, Maryland* (Sponsor: D. Livengood)

Intracellular Ca^{++} has been implicated as a regulator of various cell membrane conductances. In the present study, the Ca^{++} channel blockers Co^{++} and D600 were used to assess the role of intracellular Ca^{++} in the regulation of membrane conductances of guinea pig gallbladder epithelial cells. Addition of the Ca^{++} channel blockers to the mucosal bath reduced the intracellular potential across the apical membrane (ψ^{mc}) from −47.8 ± 4.5 to −33.0 ± 5.0 mV. The fractional resistance of the apical membrane (f_r) decreased from 0.7 ± 0.06 to 0.3 ± 0.05, whereas the transepithelial potential (ψ^{ms}) increased by 4.4 ± 1.8 mV. Since intracellular Ca^{++} has been suggested to regulate apical membrane Na conductance in several epithelia, the effect of Co^{++} on the response of ψ^{mc} and f_r to a reduction in mucosal bath Na (130 to 12 mM) was determined. In normal Ringer, reducing bath Na produced a transient hyperpolarization of ψ^{mc} with little change in f_r. In the presence of Co^{++}, the addition of low Na Ringer resulted in a sustained hyperpolarization of ψ^{mc}. These results suggest that Ca^{++} channel blockers, by decreasing intracellular Ca^{++}, increase the Na conductance of the apical membrane or, alternatively, inhibit some other transport process that normally maintains ψ^{mc} constant in spite of an apparent change in the Na conductance of the apical membrane.

64. Amiloride-sensitive Sodium Pathways in LLC-PK_1 Epithelia A. MORAN and N. MORAN, *Physiology Department, Armed Forces Radiobiology Research Institute, and National Institute of Neurological and Communicative Disorders and Stroke, National Institutes of Health, Bethesda, Maryland*

LLC-PK_1 is an established epithelial cell line derived from pig kidney that retains some characteristic properties of proximal tubule. Recently, using the patch clamp technique, we have observed in the apical membrane of these cells amiloride-sensitive sodium channels typical of a more distal part of the nephron. In the present work, we attempted to quantify the effect of amiloride on the sodium influx into the epithelium. The cells were grown in cluster-12 wells at 37°C, 5% CO_2, 95% air. Before the experiment, cells were preincubated in low (0.1–10 mM)

sodium Ringer, 0.5 mM $CaCl_2$, 4 mM K^+, and 20 mM Hepes. The influx measured either at room temperature (~25°C) or at 0°C was linear for 4 min. The amiloride dose-response curve obtained at 1 min has a $K_{0.5}$ of $\sim 2 \times 10^{-5}$ M. It is sensitive to the pH in the medium (the uptake halves when the external pH is lowered from 7.4 to 6.4). Harmaline (2 mM), another known inhibitor of Na-H exchange, completely abolishes the amiloride-sensitive flux. So does the presence of 2 mM Ca^{++}. These results are consistent with the identification of an amiloride-sensitive sodium-hydrogen antiport in the apical membrane of these cells (as shown in other preparations). The fraction of sodium flux through the amiloride-sensitive sodium conductive pathway (channels) in these cells is indistinguishable from that via the carrier, either because of the similarity of characteristics, its insignificant size, or both.

65. Convergence of α_2-Adrenergic and Muscarinic Cholinergic Mechanisms into a Common Intracellular Pathway Inhibiting Cl Secretion by the Opercular Epithelium SUSAN MAY-SZEWCZAK* and KEVIN J. DEGNAN, *Section of Physiology and Biophysics, Division of Biology and Medicine, Brown University, Providence, Rhode Island*

The rate of Cl secretion (I_{sc}) by the opercular epithelium of *Fundulus heteroclitus* is stimulated by β_1-adrenergic agonists (isoproterenol) and agents that elevate intracellular cyclic AMP (cAMP) levels (forskolin and IBMX), which indicates that β_1 agonists exert their stimulatory effect by activating adenylate cyclase. The rate of Cl secretion is inhibited by α_2-adrenergic agonists (clonidine) and muscarinic cholinergic agonists (acetylcholine [ACh]). Clonidine has been shown to exert its influence independent of cAMP levels, which indicates that it does not operate by inhibiting adenylate cyclase activity (May and Degnan, 1984, *Am. J. Physiol.*, 246(5):741). Investigations were undertaken to compare the effects of ACh on the I_{sc} and cAMP level to the known effects of clonidine on this epithelium. With the exception of efficacy, ACh mimicked the effects of clonidine in all respects. ACh inhibited the I_{sc} of control and IBMX-stimulated tissues 49.5 and 62.4%, respectively, while having no effect on the cAMP levels. Clonidine inhibited the I_{sc} of control and IBMX-stimulated tissues 86.3 and 83.3%, respectively, while having no effect on cAMP levels. In isoproterenol-stimulated tissues, ACh inhibited the I_{sc} 29.4%, while clonidine inhibited the I_{sc} 23.4%. Neither ACh nor clonidine had effects on the I_{sc} or cAMP level of forskolin-stimulated tissues. Verapamil had no effect on the inhibitory effects of ACh or clonidine on the I_{sc}. These results indicated that neither the α_2-adrenergic nor the muscarinic cholinergic mechanisms in this epithelium were mediated through inhibitory actions on adenylate cyclase. The similarities in the actions of ACh and clonidine suggest that these two different receptors may converge into a common intracellular pathway to inhibit Cl secretion. Previous studies with calcium agents (Mendelsohn et al., 1981, *J. Comp. Physiol.*, 145:29) and the lack of effect of verapamil in these studies suggest that extracellular calcium is not involved in this mechanism. [Supported by NIH grant GM 31074 to K.J.D.]

66. Effects of High Serosal K Concentrations on Electrophysiological Parameters of Frog Skin G. KLEMPERER, J. F. GARCIA-DIAZ, and A. ESSIG, *Department of Physiology, Boston University School of Medicine, Boston, Massachusetts*

In studies of apical membrane current-voltage relationships, in order to avoid laborious intracellular microelectrode techniques, epithelia are commonly exposed to high serosal K concentrations. This approach depends on the assumptions that high serosal K reduces the basolateral membrane potential and resistance to insignificantly low levels, so that transcellular values can be attributed to the apical membrane. Here we have examined the validity of these assumptions. Frog skins (*Rana pipiens pipiens*) were equilibrated in NaCl Ringer (R) solutions (110 mM NaCl, 2.5 mM KOH, 1 mM $CaCl_2$, 3.5 mM Hepes, pH 7.8), with transepithelial voltage (V_t) clamped (except for brief perturbations) at zero. The skins were impaled from the outer surface with 1.5 M KCl-filled microelectrodes (>30 MΩ). The transepithelial current (I_t) and conductance (g_t), the outer membrane voltage (V_o) (apical reference) and voltage-divider ratio ($F_o = \delta V_o/\delta V_t$), and the microelectrode resistance (R_o) were recorded continuously. Intermittent apical exposure to 20 μM amiloride permitted evaluation of cellular (c) and paracellular (p) currents and conductances. On serosal substitution of Na by K, within ~10 min, I_c [mean ± SEM (n)] declined from 27.6 ± 5.0 (3) to 13.7 ± 0.2 (4) $\mu A \cdot cm^{-2}$. g_t increased markedly as a consequence of an increase in g_p from 0.41 ± 0.18 (3) to 1.40 ± 0.20 (4) mS·

cm^{-2}. The basolateral membrane voltage V_i ($= -V_o$) was depolarized from 78 ± 4 to 2 ± 1 (4) mV, but was partially repolarized following amiloride to 6 ± 3 (4) mV. The effect of high [K] on F_o was small, with F_o changing only from 0.81 ± 0.05 to 0.87 ± 0.02 (4). This small effect is believed to be artifactual (due to the large increase in g_p), leading to an underestimation of the change in the basolateral membrane conductance (g_i). When calculated directly as the ratio of changes ($\Delta I_c/\Delta V_i$) induced by amiloride, g_i increased from 0.78 ± 0.11 to 7.65 ± 2.48 $mS \cdot cm^{-2}$. In studies employing bilateral equilibration in $NaNO_3$ R, following serosal substitution of Na by K, I_c was unchanged and g_i increased modestly from 0.87 ± 0.17 to 1.61 ± 0.18 (3) $mS \cdot cm^{-2}$. Other effects were similar to those in KCl: V_i was depolarized from 75 ± 4 to 4 ± 2 (3) mV, and F_o rose only from 0.83 ± 0.03 to 0.90 ± 0.02 (3), but g_i rose from 1.5 ± 0.06 to 6.9 ± 3.2 (2) $mS \cdot cm^{-2}$. With either serosal or bilateral equilibration in Na_2SO_4 R (plus mannitol), V_i depolarized by >40 mV from the value in NaCl R. Following serosal substitution of Na by K, V_i then depolarized from 31 ± 3 to −1 ± 1 (4) mV, F_o increased from 0.64 ± 0.01 to 0.80 ± 0.02 (4), and g_i rose from 0.26 ± 0.05 to 1.88 ± 0.59 (4) $mS \cdot cm^{-2}$. The above results demonstrate that, in the steady state, exposure to high serosal K results in essentially complete depolarization of the basolateral membrane and a large increase in its conductance. The specific influence of the above substitutions on cell K is being investigated further with K-specific microelectrodes. [Supported by USPHS grant AM 29968. G.K. is a recipient of a Cystic Fibrosis Foundation postdoctoral fellowship.]

67. Basolateral Anion and K Channels from Rabbit Urinary Bladder Epithelium J. W. HANRAHAN,* W. P. ALLES,* and S. A. LEWIS, *Department of Physiology, Yale University School of Medicine, New Haven, Connecticut*

The patch clamp technique was used to record single channel currents (both anion and K) from excised patches of the basolateral membrane of freshly dissociated rabbit bladder epithelial cells. One type of anion channel showed (in symmetrical 150 mM KCl) slight inward rectification, a slope conductance of 63 ± 6 pS at $V_M = -50$ mV, and insensitivity to Ca_i. The probability of being open at −50 mV was 0.91. From reversal potentials measured with a 5:1 KCl gradient, we estimated $P_{Cl}/P_K \geq 20$. However, *I-V* curves (measured after replacing Cl_i) indicated weak selectivity among anions; $Cl \simeq Br \simeq I \simeq SCN \simeq NO_3 >$ acetate > gluconate. A second anion channel (also found in cultured bladder cells; 1984, *Biophys. J.*, 45:300*a*) differed in its voltage dependence and conductance (370 pS), but displayed the above anion sequence. Observed less frequently was a K-selective channel having a conductance of ~200 pS in symmetrical 150 mM KCl. Although this channel did not rectify and was unaffected by Ca_i, the probability of being open increased with depolarization. At positive membrane potentials, it was blocked by Ba_i. Large basolateral conductances to K and Cl have been measured in intact bladder epithelium. The voltage-dependent K channel may serve to clamp the basolateral membrane potential during variations in transepithelial Na transport. [Supported by NSERC and MRC (Canada) fellowships and by NIH grant AM33243.]

68. Effect of Amiloride on Intracellular pH in Isolated Frog Skin K. DREWNOWSKA* and T. U. L. BIBER, *Department of Physiology and Biophysics, Medical College of Virginia, Richmond, Virginia*

Double-barreled microelectrodes were pulled from 1.5-mm theta-tubing using a horizontal micropipette puller (Industrial Science Associates). The microelectrodes were then prepared for intracellular ion activity measurements by a modification of the method described by Coles and Tsacopoulos (1977, *J. Physiol. [Lond.]*.), which permits separate perfusion of each barrel. This allowed selective silanization of one barrel by the application of a 5-min pulse of silane vapor (TMSDMA). The tip was heated at 200°C for 20 min before, during, and after the silane exposure. The conventional (nonsilanized) barrel for the cell membrane potential measurements was filled with 3.0 or 0.15 M KCl and exhibited a tip resistance of 40–60 MΩ. For the intracellular pH (pH_i) measurements, a hydrogen ion-selective liquid resin (kindly provided by Dr. Simon, ETH, Zurich, Switzerland) was introduced into the tip of the silanized barrel by using a fine glass capillary and backfilled with a buffered aqueous solution. 51% of these microelectrodes had a slope of 55.0 ± 0.6 mV/pH units. Isolated frog skins were mounted in a chamber that permitted cell punctures while the epithelium was voltage clamped. The skin was independently perfused on both sides with Ringer's solution containing 110 mM NaCl, 2.5 mM

$KHCO_3$, 1 mM $CaCl_2$, 0.2% CO_2, pH_o 7.8. The cells were impaled with the double-barreled microelectrodes from the apical bath. The pH_i was measured continuously during the application of short (typically 10 s) pulses of 10^{-4} M amiloride to the apical side. Within 2–5 min after the amiloride pulse, the pH_i decreased by 0.43 ± 0.08 pH units from a control value of 7.62 ± 0.04 (18 measurements), but then returned to 100 ± 1% of the control value within the next 2–3 min. The results are consistent with the presence of Na-H exchange at the apical side of the epithelial cells. [Supported by NIH grant AM 26347.]

69. Glutaraldehyde Fixation of Sodium Transport in Dog Red Blood Cells JOHN C. PARKER, *University of North Carolina at Chapel Hill, Chapel Hill, North Carolina*

The large increase in passive Na flux that occurs when dog red blood cells are caused to shrink is amiloride sensitive, associated with a reciprocal movement of protons, and inhibited when chloride is replaced by nitrate or thiocyanate. Activation and deactivation of this transport pathway by manipulation of cell volume is reversible. Brief treatment of the cells with 0.01–0.03% glutaraldehyde can cause the shrinkage-activated transporter to become irreversibly activated or inactivated, although the cells will continue to be osmometers. Thus, if glutaraldehyde is applied when the cells are shrunken, the amiloride-sensitive Na transporter is activated and remains so regardless of subsequent alterations in cell volume. If the fixative is applied to swollen cells, no amount of subsequent shrinkage will turn on the Na pathway. In its fixed state, the activated transporter is fully amiloride sensitive, but it is no longer inhibited when chloride is replaced by thiocyanate. The action of glutaraldehyde thus allows one to dissect the response to cell shrinkage into two phases. Activation of the pathway is affected by anions and is not prevented by amiloride. Once activated and fixed, the anion requirement disappears. Amiloride inhibits movement of Na through the activated transporter. These experiments demonstrate how a chemical crosslinking agent may be used to study the functional properties of a regulable transport pathway.

70. Passive Cation Movements Through the Sodium Pump in Human Red Blood Cells LINDA J. KENNEY and JACK H. KAPLAN, *Department of Physiology, University of Pennsylvania, Philadelphia, Pennsylvania*

We recently reported that ADP will support ouabain-sensitive P_i-dependent K:K exchange in resealed red cell ghosts (1982, *Ann. NY Acad. Sci.*, 402:292). Closer examination of these fluxes revealed a small ouabain-sensitive flux in the absence of ADP. Karlish and Stein (1982, *J. Physiol.* [*Lond.*]., 328:295) have described small fluxes mediated by the purified Na,K-ATPase after detergent treatment and incorporation into proteoliposomes. We have extended our studies of the ADP-independent and P_i-independent ouabain-sensitive ^{86}Rb uptake in resealed red cell ghosts and find that: (*a*) in the absence of ADP (or ATP), P_i or AsO_4 supports Rb:Rb exchange with both activating and inhibitory phases; (*b*) in the absence of P_i, ADP activates and at higher concentrations inhibits Rb:Rb exchange; (*c*) in the absence of P_i and ADP, ouabain-sensitive Rb:Rb exchange is small but measurable, other cations will substitute for Rb at the cytoplasmic surface (Li, Cs, K), and Rb at the extracellular surface activates with a $K_{0.5}$ of <500 μM. Although these fluxes are too small to be significant physiologically, their characterization in red cells establishes their relevance to the operation of sodium pumps in their normal membrane environments. [Supported by NIH grant HL30315. J.H.K. is a recipient of RCDA K04HL01092. L.J.K. is supported by Cell and Molecular Biology Training Grant 5T-32-GM07229.]

71. Na^+-K^+ Cotransport in Human Red Cells: Reversible Inactivation by Metabolic Depletion N. C. ADRAGNA, C. M. PERKINS,* and P. K. LAUF, *Department of Physiology, Duke University Medical Center, Durham, North Carolina*

About half of the ouabain-resistant (OR) Na^+ and K^+ fluxes in human red cells is ascribed to furosemide-sensitive (FS) Na^+-K^+ cotransport, which may be measured as zero-*trans* cation efflux into isosmotic $MgCl_2$-sucrose solutions or as Na^+-dependent K^+ (Rb^+) influx. In 1971, Beauge and Adragna (*J. Gen. Physiol.*, 57:577) showed that the latter was inhibited by iodoacetamide and hence inferred its metabolic dependence. Here we extend this earlier work by

employing a technique to reversibly deplete human red cells of their intracellular ATP, $(ATP)_c$, and to study its effect on OR and FS zero-*trans* Na^+-K^+ effluxes under V_{max} conditions. Human red cells were cation loaded for 20 h using PCMBS to permeabilize temporarily the membrane to cations. Cells containing ~80 and 50 mmol K^+ and Na^+/liter cell water, respectively, were resealed with 4 mM cysteine, and $(ATP)_c$ was restored by 1 h incubation in a cocktail containing (mM): 3 inosine, 2 adenine, 10 glucose, and 2.5 P_i. Metabolic depletion was achieved by incubation for up to 8 h in 10 mM 2-deoxy-D-glucose in the presence of EGTA, and subsequently reconstituted with ATP by exposure to 10 mM glucose plus 5 mM inosine over 3 h at 37°C. We found that total OR Na^+ and K^+ fluxes increased ~20% or more in metabolically depleted cells [$(ATP)_c$ = 54 μM/liter cells]. Furosemide-insensitive (FI) Na^+ and K^+ fluxes increased ~100%, with a concomitant complete loss of FS Na^+ efflux but only a 60% reduction of FS K^+ efflux. In ATP-repleted cells [$(ATP)_c$ = 1.1 mM/liter cells], all the components of Na^+ and K^+ fluxes returned to baseline levels, with the exception of total OR Na^+ efflux, which remained slightly elevated. The following conclusions can be drawn: (*a*) FS Na^+ effluxes were more sensitive to ATP depletion than FS Na^+-K^+ fluxes; (*b*) FI Na^+ and K^+ fluxes increased as FS fluxes fell after ATP depletion, which suggests a metabolically dependent, functional interconvertibility of FS and FI cation fluxes or an effect of ATP depletion on the inhibitory action of furosemide; (*c*) the effects on OR FS and FI Na^+ and K^+ fluxes induced by metabolic depletion were reversible. Although a 9% swelling was observed in cells depleted as described above, the induced "uncoupling" of FS Na^+ and K^+ efflux cannot be explained by this fact since cells metabolically depleted in the absence of EGTA were similarly swollen (6%) and with equally low $(ATP)_c$, but the FS Na^+ and K^+ fluxes were not uncoupled and were reduced by only 20% with respect to controls. Hence, in order to abolish FS Na^+ efflux and to cause an apparent "uncoupling" from the more stable FS K^+ fluxes, ATP depletion plus bivalent metal chelation is required. [Supported by NIH grant AM 28236.]

72. Evidence for the Conformation of Band 3 Protein in Which the Single Proton and Anion Cotransport Sites Are Opposed, i.e., They Face Opposite Sides of the Membrane at the Same Time

R. B. GUNN, *Department of Physiology, Emory University School of Medicine, Atlanta, Georgia*

The band 3 protein of human erythrocyte membranes mediates cotransport of protons and anions and rapid anion exchange. *cis* protons are mixed inhibitors of *cis* activation by chloride of chloride exchange, M, on both the inside and outside separately (Milanick and Gunn, manuscript submitted for publication). Dixon graphs (1/M vs. H^+) are linear for H_i and H_o. Thus, a single proton inhibitory site, separate from the anion binding site, exists on both sides of the membrane. The pK for the activation of proton-sulfate cotransport (5.5) is nearly the same as the pK's for inhibition of chloride flux (5.0–6.0) (Milanick and Gunn, 1984, *Am. J. Physiol.*); thus, the simplest model consistent with the data requires only a single proton binding and transport site in the pH range 4.0–8.5. Three types of experiments suggest that the proton transport site and anion transport site can face opposite solutions at the same time. Thus, it may be possible that cotransport involves the transport of first one ion and then the other, rather than the simultaneous cotransport of both. First, the ratio of $V_{max\text{-}out}/K_{\frac{1}{2}\text{-}out}$, determined by Cl_o activation curves at fixed Cl_i and pH_o, is decreased by H_i with a pK of 6.1 (Milanick and Gunn, manuscript submitted for publication). Second, the initial rate of sulfate efflux/chloride influx at fixed pH_i is >90% inhibited by H_o. Third, sulfate influx at fixed pH_i is only activated by increasing H_o if the cells contain only chloride, but is activated and then inhibited if the cells contain only sulfate. This opposed conformation of the protein provides a simple explanation for these experiments and for (*a*) self-inhibition and (*b*) sigmoid activation kinetics at very low pH values. The model consists of a single anion transport site, a single proton transport site, and the existence of the opposed conformation of these two sites. [Supported in part by USPHS grant HL 28674.]

73. Computer Program to Generate the Steady State Transport Equation for Any Kinetic Scheme

V. K. GOTTIPATY* and R. B. GUNN, *Department of Physiology, Emory University School of Medicine, Atlanta, Georgia*

A computer program written in BASIC has been developed to solve analytically, not numerically, any steady state chemical reaction scheme. This program solves the kinetic scheme

using Wang algebra and is equivalent to the King-Altman method or the steady state solution of the differential equations. The program generates terms that are sums of products of individual rate coefficients, product concentrations, and substrate concentrations, for the steady state fractional concentration of each intermediate in the reaction scheme. The flux equation for a transport reaction can then be written directly in complete detail. To use the program, one writes out the scheme and makes a representation that shows all the transporter (enzyme) species and the allowed reactions between them. Each species is given a number and each forward and reverse reaction is given a rate coefficient name. The program asks for the number of species, n, all pairs of rate coefficients for reactions leaving each transporter species, and a list of the rate coefficients leading to and from each separate species. The first output is the list of all the sums of products of rate coefficients for all species, which is the denominator for the fractional steady state concentration of every species. The second output is the list of the sums of products of rate coefficients, which form the numerator for any desired species. The program can sort the output expressions in terms of given rate coefficients or combinations of rate coefficients. Thus, if the second-order rate coefficient k_1 is to be replaced by the pseudo–first-order rate constant k_1S, all of the terms with k_1 can be segregated in the printout of both the numerator and the denominator expressions. This sorting allows one to write easily the phenomenological equation by inspection without the detailed rate coefficients, e.g., flux = $(AS + BS^2)/(CS + DS^2 + ES^3)$, where $A, B \ldots E$ are the sorted sums of products of rate coefficients and inhibitor concentrations (if any) and S is the substrate concentration. [Supported in part by USPHS grant HL 28674.]

74. Cation Transport in Hemoglobin CC Red Blood Cells CARLO BRUGNARA,* ALAN KOPIN,* H. FRANKLIN BUNN,* and DANIEL C. TOSTESON, *Department of Physiology and Biophysics and Department of Medicine, Brigham and Women's Hospital, Harvard Medical School, Boston, Massachusetts*

The aim of this study is to investigate how the reduced cation (and water) content of CC cells is related to different cation transport properties of CC cells. The maximal rates of the Na-K pump (measured as ouabain-sensitive Na efflux from cells with $Na_i = K_i = 50$ mmol/liter cell) and of the Li_i-Na_o exchange (measured as Na_o-stimulated Li efflux) were significantly higher in CC than in control cells. However, the maximal rate of outward Na-K cotransport (measured as bumetanide-sensitive Na and K efflux into choline 1 mg medium) was lower in CC than in control. Compared with control cells, CC cells incubated in the presence of both ouabain and furosemide had 2.5 times higher Na efflux and influx and 5.5 and 15 times higher K efflux and influx, respectively. K efflux from CC cells in the presence of both ouabain and bumetanide (OB) rose from 5–6 to 20–25 mmol/liter cell·h (FU), when cell volume was increased by exposure to hypotonic media or by increasing cell solute content (nystatin method). When CC cells were incubated in hypotonic medium with ouabain and bumetanide, they shrank toward the original volume. No volume changes were observed in control cells. In CC cells, the dependence of OB-resistant K efflux on pH_o had a bell shape, with a maximal flux (20–25 FU) at pH 6.9. In contrast, the K efflux from control cells was minimal at pH 7.4 (1.2 FU) and was slightly stimulated by acid and alkaline pH. In order to study the effect of pH_i and pH_o on the OB-resistant K efflux, CC cells were incubated with DIDS (150 μM) and acetazolamide (1 mM) at different pH_i (6.7, 7.3, and 7.8), and resuspended in media with different pH_o (6.75, 7.4, and 8). The OB-resistant K efflux was stimulated by acid pH_i and was independent of pH_o. The OB-resistant K efflux from CC cells was not inhibited by Mg_o (0–20 mM), quinine (75 μM), carbocyanin (10 μM), or trifluoroperazine (10 μM). Similarly, K efflux from CC cells was unchanged when measured into a medium containing the ionophore A21387 and EGTA. Amiloride (1 mM) inhibited 20% of the K efflux under basal conditions and under volume- or pH-stimulated conditions. Thus, the reduction in water and K content of CC cells is probably related to an increased movement of K through a ouabain- and bumetanide-resistant pathway that is volume and pH_i dependent. It remains to be determined how the genetically determined abnormality in the primary structure of hemoglobin C leads to such a modification in cation transport.

75. A Method to Select Membrane Transport Mutants in Epithelial Cell Cultures by Tritium Suicide and Replica Plating: Application to the Active Sugar Transporter of

LLC-PK$_1$ Cells JAMES M. MULLIN,* EDWARD A. ADELBERG,* and CAROLYN W. SLAYMAN, *Department of Human Genetics, Yale University School of Medicine, New Haven, Connecticut*

Transport-defective mutants can be selected by exposing mutagenized cells to tritiated substrate and then freezing the cells at −70°C. Normal cells thereupon undergo tritium suicide, while transport-defective mutants survive. Thawing and plating the survivors provides a set of clones in which the desired class of mutants has been so enriched that their detection is possible by replica plating. LLC-PK$_1$ cells possess an active sugar transporter for which alpha-methyl-D-glucoside (AMG) has high affinity. It should thus be possible to select transport-defective mutants by incubating mutagenized cells with [^{3}H]AMG, allowing them to undergo tritium suicide, replica plating the survivors, and testing the replicas for transport by autoradiography. The following properties of LLC-PK$_1$ cells demonstrate the feasibility of this approach: (*a*) the cells grow (and form domes) in medium in which glucose is replaced by fructose; thus, loss of the transporter in question should not be lethal; (*b*) the frequency of ouabain-resistant mutants is increased 10-fold by treating the cells with 500 μg/ml ethylmethanesulfonate for 18 h; thus, mutagenesis is effective; (*c*) [^{3}H]AMG can be sufficiently accumulated by the cells to kill >95% of the population during 30 d storage at −70°C; (*d*) clones of cells growing in culture dishes can be replicated into polyester cloth using the method of Raetz et al. (1982, *Proc. Natl. Acad. Sci. USA*, 79:3223); replicas possess active sugar transport as detected by [^{14}C]AMG autoradiography. While these experiments demonstrated the potential feasibility of tritium suicide to select for mutants defective in active sugar transport, they have revealed several interesting properties of LLC-PK$_1$ cells: (*a*) dome formation occurs in fructose medium, which indicates an apical Na^+ current independent of Na-sugar cotransport; (*b*) the transporter is expressed in the replicas, dissociating differentiation from confluence; (*c*) the tritium suicide curve is biphasic, which indicates that confluent cultures are heterogeneous regarding active sugar transport.

76. Effect of Calcium Blockers on I_{Ca} and E-C Coupling in Frog Twitch Muscle H. GONZALEZ-SERRATOS,* R. VALLE-AGUILERA,* and ANN WILLIAMSON,* *Department of Biophysics, University of Maryland, Baltimore, Maryland; Department of Pharmacology, Universidad de San Luis Potosi, Mexico*

The present experiments were designed to see if the Ca blockers diltiazem and verapamil affect some I_{Ca} and mechanical properties that will reflect changes in E-C coupling steps. In fibers mounted in a vaseline gap voltage clamp system, it was found that (*a*) the 100% recovery time of I_{Ca} is 1.5–1 min; (*b*) between 2 and 6 s after the first pulse, I_{Ca} is still completely inactivated; and (*c*) different frequencies of depolarization (1–0.3/min) produce a larger and continuous decline of I_{Ca} magnitude. On fresh isolated cells, diltiazem (3×10^{-6} M) potentiates twitch tension (up to 2.5 times) with prolongation of the half-relaxation time (1.9 times). Partially fused tetanus are potentiated and maximal tetanic tension is not affected. Verapamil (1×10^{-6} M) has a smaller potentiating effect. K contractures (1–20°C) and redevelopment of tension after their interruption were not affected by either drug. In a third group of experiments, both I_{Ca} and mechanical activation were investigated in the same cut fiber preparation before and after perfusing the cell with either one of the drugs. In the presence of the drug, mechanical activation caused by I_{Ca} could not be stopped unless I_{Ca} had decreased substantially. Mechanical activation caused by brief (50–70 ms) depolarizations remained even after I_{Ca} had disappeared. [Supported by NIH grant NS17048-02S1, by the American Heart Association (Maryland Affiliated), and by SEP 8504474Y0101 to R.V.A.]

77. Intracellular Free Ca^{2+} and Its Possible Link to Na Pump Activity in Single Smooth Muscle Cells H. YAMAGUCHI,* *Department of Physiology, University of Massachusetts Medical School, Worcester, Massachusetts*

Intracellular Ca^{2+} activity (A_{Ca}) in single smooth muscle cells isolated from toad stomach was measured by single- and double-barreled Ca^{2+}-selective microelectrodes. They were produced from aluminosilicate glass micropipettes containing a short column (75–100 μM) of the neutral Ca ligand. Double-barreled Ca^{2+} electrodes, however, required fusing three pipettes to obtain a resistance $>10^{13}$ Ω between recording pipettes. Both types of electrodes had Nernstian responses to below 10^{-7} M A_{Ca}, with slopes of 28–30 mV and detection limits at or below 10^{-8}

M A_{Ca}. Impalement of smooth muscle cells with the single-barreled Ca^{2+} electrodes gave two populations of DC potentials; some cells stayed relaxed upon penetration; these averaged -171.4 ± 7.73 mV (SEM, $n = 6$). Other cells contracted and averaged -113.6 ± 2.93 mV ($n = 4$). Subtracting the membrane potential (E_m: -56.4 mV), these figures can be expressed as $A_{Ca} = 5.5 \times 10^{-8}$ M and 5.4×10^{-5} M, respectively. Observations with double-barreled Ca^{2+} electrodes indicated that intracellular A_{Ca} was fairly constant in response to step changes of E_m caused by elevation of $[K^+]_o$. In contrast, a steady rise of A_{Ca} was observed after exposure to ouabain. A ouabain-sensitive hyperpolarization (induced by a sudden change from high K^+ to normal K^+) resulted in a significant reduction of intracellular A_{Ca}. These results suggest that intracellular Na^+ may play an important role in regulating intracellular Ca^{2+}. [Supported by grants from Smokeless Tobacco Research Council and the NSF.]

78. Identification of Functional β-Adrenergic Receptors on Intact Smooth Muscle Cells J. L. CONKLIN* and F. S. FAY, *University of Massachusetts, Worcester, Massachusetts*

To investigate early events linking β-adrenergic (β) receptor stimulation with its inhibitory effect on smooth muscle cell (SMC) contraction, we have characterized the binding of the β-antagonist (±)[^{3}H]CGP-12177 (CGP) to β receptors on freshly isolated, intact SMCs. Contraction of these SMCs is inhibited by (−)isoproterenol (ISO), and this response is blocked by (−)pindolol (PIN) (K_I = 790 pM). At equilibrium binding, SMCs had 7,900 specific and saturable CGP binding sites/cell (K_D = 370 pM). The K_D determined from k_{-1} and k_{+1} was 350 pM. Binding was stereoselective since (−)ISO was nearly 50 times more potent than (+)ISO in inhibiting CGP binding. CGP binding sites correspond to functional β receptors since PIN blocks CGP binding (K_I = 680 pM) and β stimulation of SMCs (K_I = 790 pM) with essentially the same potency. Unexpectedly, (−)ISO was nearly 100 times more potent an inhibitor of contraction than of CGP binding. Computer-assisted analysis of the (−)ISO binding inhibition curve demonstrated high- and low-affinity sites for ISO binding. This observation, together with the demonstration that the inhibitory effects of ISO on SMC contraction decline with continued ISO exposure, suggests that β-adrenergic agonist-induced desensitization may be due to a decrease in β receptor affinity for agonist. Studies exploring this hypothesis are ongoing. [Supported by NIH grants HL-06667-01 and 14523-12.]

79. Voltage Dependence of Calcium Release and Intramembrane Charge Movement in Frog Skeletal Muscle G. SZUCS,* B. SIMON,* and M. F. SCHNEIDER, *Department of Physiology, University of Rochester, Rochester, New York*

We have measured both the rate of SR calcium release (Melzer et al., 1984, *Biophys. J.*, 45:637) and intramembrane charge movement (Horowicz and Schneider, 1981, *J. Physiol. [Lond.].*, 314:565) in single cut twitch muscle fibers at ~5–8°C using a double vaseline gap voltage clamp (holding potential = −100 mV). Charge movement (Q) could be determined for pulses to voltages ranging from −80 to +20 mV and was well fit by the two-state Boltzmann relationship $Q/Q_{max} = 1/\{1 + \exp[(\bar{V} - V)/k]\}$, with mean $\bar{V} = -28$ mV and mean $k = 22$ mV. In the same three fibers, Ca release was undetectable at voltages negative to −40 or −50 mV. For more positive voltages up to +40 or +60 mV, the peak rate of Ca release was fit by the Boltzmann relationship with mean $\bar{V} = -6$ mV and mean $k = 12$ mV. Thus, both Q and peak rate of Ca release approach maximum values over a similar positive voltage range. Around the threshold voltage for calcium release, the measured peak rate of release fell below the fit of the Boltzmann relationship, increasing e-fold for a 5-mV increase in V (same three fibers). The value of Q at the threshold voltage for Ca release was taken to be the threshold charge movement, Q_{th}, for Ca release. The suprathreshold charge, $Q - Q_{th}$, was calculated and found to follow the same voltage dependence as the peak rate of calcium release. Thus, the rate of Ca release may be governed by the amount of suprathreshold charge moved at each voltage. [Supported by grants from the MDA and NIH.]

80. External Ca-dependent Na Efflux ("Reversed" Na/Ca Exchange) in Single Barnacle Muscle Cells H. RASGADO-FLORES,* E. M. SANTIAGO,* and M. P.

BLAUSTEIN, *Department of Physiology, University of Maryland School of Medicine, Baltimore, Maryland*

The Na/Ca exchanger-mediated (net) movements of Na and Ca across the plasmalemma should be governed by the membrane potential and the Na and Ca concentration gradients. However, it has been reported that in squid axons, the "reverse" mode of exchange (Ca influx/Na efflux) may not be a simple symmetrical reversal of the "forward" mode (Na influx/Ca efflux) because internal Na-dependent Ca influx and external Ca (Ca_o)-dependent Na efflux require intracellular Ca and ATP (DiPolo, 1979, *J. Gen. Physiol.*, 73:91; Baker and Allen, 1984, *In* Abstr. Symp. on Calcium and Phosphate Transport Across Biomembranes, Bronner and Peterlik, editors, 1–2). We studied Ca_o-dependent ^{22}Na efflux in internally perfused giant barnacle muscle cells. The internal perfusion fluid contained (mM): 40 Na glutamate, 38 KCl, 162 K glutamate, 285 sucrose, 7 $MgCl_2$, 60 HEPES (pH 7.3), 8 EGTA without or with 3.44 $CaCl_2$ (to obtain 0.1 μM free Ca), and 3 U/ml apyrase, or 3 MgATP plus 1.5 phosphoenolpyruvate and 0.08 mg/ml pyruvate kinase. The external fluid contained (mM): 456 LiCl, 10 KCl, 25 $MgCl_2$, 11 $CaCl_2$, 6 Tris (pH 7.8). In ATP-fueled cells, 0.1 mM ouabain reduced Na efflux significantly; replacing Ca_o with Mg reversibly reduced Na efflux further and reversibly depolarized the cells. In ATP-depleted cells, ouabain had no effect, but Ca_o replacement still reduced Na efflux and produced a depolarization. The Ca_o-dependent Na efflux was also observed in the presence of ATP and in the virtual absence of intracellular Ca. This Ca_o-dependent Na efflux was generally larger in depolarized fibers (V_M less than −30 mV) even when the external media contained NaCl rather than LiCl. Increasing external K also increased the Ca_o-dependent Na efflux; this could be a direct result of K itself, or a consequence of membrane depolarization. Voltage clamp experiments are planned to test this directly. The results are consistent with a symmetrical Na/Ca exchanger able to transport Na and Ca in either direction in barnacle muscle cells. [Supported by the MDA and NIH grant AM-32276.]

81. A Delayed Calcium Influx Related to Contraction in Frog Twitch Fibers

B. A. CURTIS and R. S. EISENBERG, *Departments of Physiology, University of Illinois College of Medicine at Peoria, Peoria, Illinois; Rush Medical School, Chicago, Illinois*

Calcium uptake by isolated frog muscle fibers soaked in 30 μM D600 at 3–5°C was measured by counting radioactive disintegrations from the center of the fiber following a period of ^{45}Ca influx. Fibers soaked in ^{45}Ca for 3 min before application of elevated K (containing ^{45}Ca) for 2 min took up 7.1 ± 0.9 (27) pmol Ca/fiber. After one K contracture in D600, fibers were unable to contract in response to K depolarization (despite normal resting and action potentials and caffeine contractures) and took up 3.8 ± 0.7 (16) pmol Ca/fiber. The paired difference was 2.9 ± 0.8 (16) pmol Ca/fiber, a Ca influx related to contraction. All fibers contracted after warming. Nickel added to D600 reduced the Ca influx in paralyzed fibers to 1.3 pmol/fiber (resting) and in contracting fibers to 2.1 ± 0.4 pmol. The difference in Ca uptake between fibers contracting in D600 and Ni-D600 represents a voltage-sensitive component of calcium unrelated to contraction of 1.5 pmol/min. ^{45}Ca added to K after relaxation entered in the same amount as the contraction-sensitive component and may be refilling an internal Ca store emptied in the preceding contracture. When the contracture inducing 190 mM K was rapidly flushed away and ^{45}Ca was added to the Na Ringer for 5 min, a contracting fiber took up 2.2 pmol Ca. When the fiber was paralyzed in 30 μM D600, it took up 0.8 pmol. Correction for resting influx gives 1.48 and 0.08 pmol, respectively. We believe this delayed, contraction-sensitive Ca uptake, 2–3 pmol/contracture, refills an internal store (possibly on the cytoplasmic surface of the t-tubule wall), emptied to initiate the preceding contracture. This Ca entry might be the rate-limiting step in return of contractile ability. [Supported by NIH grant HL-20230.]

82. Muscarinic Stimulation of Single Smooth Muscle Cells Causes a K^+ Conductance Decrease

STEPHEN M. SIMS,* JOSHUA J. SINGER, and JOHN V. WALSH, JR., *Department of Physiology, University of Massachusetts Medical School, Worcester, Massachusetts*

Cholinergic responses were studied in single, freshly dissociated smooth muscle cells from the stomach of the toad *Bufo marinus*, using single electrode current and voltage clamp techniques. Acetylcholine or muscarine caused slow depolarization, sometimes giving rise to action potentials and contractions. We interpret the cholinergic depolarization as being due to

the closure of K^+ channels, basing this conclusion on the following evidence. (*a*) Depolarization was accompanied by a conductance decrease, seen as increased voltage deflections in response to constant current pulses. (*b*) The conductance decrease was confirmed under voltage clamp conditions. Steady state current deflections in response to constant voltage commands were smaller in the presence of cholinergic agonists. (*c*) The K^+ dependence of the cholinergic responses was demonstrated by raising $[K^+]_{out}$ (replacing Na^+) from the usual value of 3 to 20–90 mM, thereby shifting E_K into the range of voltages in which this voltage-sensitive g_K was activated (see below). The currents induced by muscarine reversed direction near the expected values of E_K. The estimated reversal potentials of muscarine-induced currents were dependent upon $[K^+]_{out}$, shifting 57 mV positive per 10-fold elevation of $[K^+]_{out}$. The I_K suppressed by cholinergic agonists is similar to the M current of sympathetic neurons. Hyperpolarizing voltage commands resulted in slow current relaxations, which reflects the closing of K^+ channels. Cholinergic agonists abolished the current relaxations. Thus, cholinergic stimulation of smooth muscle cells appears to depress this voltage-sensitive K^+ current. The existence of a cholinergic conductance decrease is of interest because it has heretofore gone unrecognized in smooth muscle. [Supported by NSF grants PCM-7904938 and PCM-8208015, and by NIH grant AM 31620. S.M.S. was supported by MRC Canada.]

83. Paradoxical Effect of La^{+++} Ions on the Response of Cultured Cardiac Cells to Na Withdrawal R. HARDWIN MEAD* and WILLIAM T. CLUSIN, *Cardiology Division, Stanford University, School of Medicine, Stanford, California*

When chick embryonic myocardial cell clusters are voltage clamped in the pacemaker range, abrupt removal of external Na causes the following: (*a*) an early outward current caused by interruption of background Na influx; (*b*) a late inward current caused by a nonspecific conductance increase; (*c*) spontaneous asynchronous mechanical activity (Mead and Clusin, 1984, *Circ. Res.*, in press). Effects *b* and *c* may depend upon influx of Ca through the Na/Ca exchange. Accordingly, we compared the effects of three agents that reputedly block Na/Ca exchange on the Na withdrawal response. 90–130-μM-diam cell clusters were clamped between −50 and −90 mV using a single-electrode voltage clamp. Uniformity of membrane potential control was verified by a second impalement (Clusin, 1983, *Nature* [*Lond.*]., 301:248). Pretreatment with Mn^{++} ions (25 mM) prevented the mechanical response, the late inward current, and the conductance increase during Na removal. The early outward current was reduced by 27 ± 10%, but was not abolished. Adriamycin (25–50 μM) had similar effects. In contrast, La^{+++} ions (1 mM) caused a paradoxically opposite response. La^{+++} accentuated the mechanical activity during Na removal, and reduced its latency of onset from 8.9 ± 3.8 s <1 s. The nonspecific conductance increase was two- to fourfold larger in La^{+++}, and the time constant with which it developed increased from a usual value of 19 ± 6 to 3 ± 2 s ($P < 0.001$, $n = 5$). In some records, the nonspecific conductance increase was rapid enough to completely obscure the initial outward current. We conclude that Mn^{++} and adriamycin have effects consistent with block of Na/Ca exchange. Since La^{+++} also blocks Na/Ca exchange (Barry and Smith, 1982, *J. Physiol.* [*Lond.*]., 325:243), its surprising electromechanical effects may be due to release of sequestered intracellular calcium. [Supported by NIH grant 1 R01 HL 32093-01, by postdoctoral fellowship 1 F32 HL 06761-01 to R.H.M., and by an American Heart Association Established Investigator Award to W.T.C.]

84. Effects of Spermine in Skinned Cardiac Cells Suggest That Mitochondria Do Not Participate in Beat-to-Beat Ca^{2+} Regulation in Intact Cardiac Cells but Control Caffeine-induced Contracture and Might Regulate Resting [Free Ca^{2+}] ALEXANDRE FABIATO, *Department of Physiology, Medical College of Virginia, Richmond, Virginia*

The previous conclusion that mitochondria play no role in the cytosolic Ca^{2+} regulation of cardiac muscle (Fabiato, 1983, *Am. J. Physiol.*, 245:C1) should be reconsidered after the demonstration by Nicchitta and Williamson (1984, *J. Biol. Chem.*, in press) that spermine strongly enhances the affinity of liver mitochondria for Ca^{2+}. Spermine is a polyamine present at a total concentration of ~2 mM in the intact cardiac cell, but the free concentration is unknown. The experiments were done in skinned (sarcolemma removed by microdissection) single cardiac cells from the rat ventricle. The control solution contained 0.068 mM total

EGTA, pMg 2.70, pMgATP 2.50, pH 7.10 buffered with 30 mM *N,N*,bis(2-hydroxyethyl)-2-aminoethanesulfonic acid, 12 mM phosphocreatine with 15 U/ml creatine phosphokinase, 1 mM pyruvate, 1 mM malate, 5 mM glutamate, and 120 mM KCl (no Na^+). Adding 0.8 mM spermine decreased from 2.00 to 0.32 μM the [free Ca^{2+}] necessary for loading the mitochondria to a level permitting the substitution of 20 mM NaCl for 20 mM KCl to induce a detectable tension transient caused by Ca^{2+} release from the mitochondria. The steady state [free Ca^{2+}] required for obtaining spontaneous cyclic contractions by overload of the sarcoplasmic reticulum (SR) was increased from 0.10 to 1.78 μM in the presence of 0.8 mM spermine. This might suggest that the mitochondria regulate the resting [free Ca^{2+}] in the intact cell by preventing the Ca^{2+} overload of the SR. However, the Ca^{2+} accumulated in the mitochondria does not seem to be rapidly releasable. When the skinned cells were exposed to >0.32 μM free Ca^{2+}, they deteriorated, probably because of Ca^{2+} overload of the mitochondria inhibiting their respiration. The phasic contraction induced by 10 mM caffeine, which is caused by Ca^{2+} release from and very slow reaccumulation in the SR, was dramatically curtailed by the addition of 0.8 mM spermine. Hence, spermine increased the rate of Ca^{2+} accumulation of the mitochondria to a level permitting them to sequester Ca^{2+} during this long-lasting contraction. In contrast, 0.8 mM spermine did not modify the potentially physiological Ca^{2+}-induced release of Ca^{2+} elicited by a rapid change of [free Ca^{2+}] at the outer surface of the SR: the [Δfree Ca^{2+}]/Δt requirement was not modified, and the duration and amplitude of the resulting phasic contraction were unchanged because the phasic contraction was too brief to permit significant Ca^{2+} accumulation by the mitochondria. [Supported by NIH grant R01 HL19138.]

85. (K + Cl) Co-Transport in Cultured Chick Heart Cells

D. PIWNICA-WORMS, R. JACOB,* C. R. HORRES, and M. LIEBERMAN, *Department of Physiology, Duke University Medical Center, Durham, North Carolina*

The polystrand preparation of cultured chick heart cells has been characterized as having a unidirectional transmembrane Cl efflux that is twice K efflux (1983, *J. Gen. Physiol.*, 81:731). Because the Cl conductance of this heart cell membrane is low (irrespective of K_o), this suggests the existence of electroneutral Cl-dependent transport mechanisms. Furosemide (10^{-5} M) decreases the ^{36}Cl tracer efflux rate constant from a control value of 0.67 min^{-1} to 0.33 min^{-1}. 133 mM K_o solution also reduces the ^{36}Cl efflux rate constant, in this case to 0.14 min^{-1}; Na_o-free solution, which depletes Na_i within 1 min, has no significant effect on Cl efflux. K_o-free solution, in the presence of DIDS (10^{-4} M) to prevent Cl movements through anion exchange, results in intracellular Cl content loss and volume decrease; Cl is driven against its electrochemical gradient and the loss is furosemide sensitive in a dose-dependent manner. Initial equalization of internal and external K by incubating polystrands in 133 mM K_o, 128 mM Cl_o solution for 20 min causes net K and Cl uptake in a 1:1 stoichiometry, as well as a furosemide-sensitive volume increase; high $choline_o$ or Li_o cannot mimic this high K_o-induced volume increase. Removal of Cl_o from 133 mM K_o solution prevents K uptake and causes Cl loss, as well as a furosemide-sensitive volume decrease. Adjusting external Cl concentrations in high K_o solution plus DIDS (0.5×10^{-4} M), such that the Cl chemical gradient equally opposes the K chemical gradient, prevents high K_o-induced volume changes. These data indicate that the cardiac cell membrane contains a furosemide-sensitive (K + Cl) co-transport mechanism. [Supported by NIH grants HL 07101, HL 27105, and GM 07171.]

86. Electrogenic Na/Ca Exchange in Cultured Heart Cells

R. JACOB,* S. LIU,* E. MURPHY, and M. LIEBERMAN, *Department of Physiology, Duke University Medical Center, Durham, North Carolina*

A direct demonstration of the electrogenicity of the Na/K pump has been its ability to hyperpolarize the membrane potential (E_m) beyond the most negative ionic reversal potential. There has been no such demonstration for Na/Ca exchange in intact cardiac muscle despite several reports of it being electrogenic. When strands of cultured chick embryo heart cells were exposed to 10^{-4} M ouabain in K_o = 0 or 5.4 mM, E_m depolarized to −40 mV. After 3 min of ouabain exposure, the strands were exposed to low Na_o (nominally 30 mM, TMA substitute) and E_m hyperpolarized by ~25 mV, i.e., not beyond the potassium reversal potential (E_K). To reduce the difference between E_m and E_K, the experiment was repeated in K_o = 24 mM (+10^{-4} M ouabain): E_m after 3 min was −37.7 ± 0.6 mV (± SEM, n = 3) and exposure to low Na_o hyperpolarized E_m to −41.6 ± 1.2 mV (n = 3). However, E_K (measured separately using ion-

selective microelectrodes) in K_o = 24 mM ($+10^{-4}$ M ouabain) was -47.0 ± 0.3 mV ($n = 7$), i.e., still negative to E_m. In the same experiment on monolayer cultures, exposure to low Na_o raised the Ca content and lowered the Na content against the Na electrochemical gradient, which suggests a gradient-coupled movement of Na ions associated with the hyperpolarization. To reduce any potassium shunt pathway, 1 mM Ba^{2+} was added 1 min before and during exposure of the strands to low Na_o. Addition of Ba^{2+} depolarized E_m to -32.5 ± 2.3 mV ($n = 3$), but exposure to low Na_o now caused a large hyperpolarization to -62.3 ± 1.5 mV ($n = 3$), which was significantly negative to E_K ($P < 0.0005$). Also, E_{Na} in these circumstances was well positive to E_m. To eliminate possible involvement of residual unbound Na/K pump sites, the experiment was repeated raising [ouabain] to 1.1×10^{-3} M on addition of Ba^{2+}: E_m hyperpolarized to -57.3 ± 1.5 mV ($n = 3$), still significantly negative to the above value of E_K ($P < 0.0005$). Repeating the experiment with simultaneous measurements of E_K and the hyperpolarization in low Na_o showed that E_m hyperpolarized significantly beyond E_K by 17.0 ± 2.9 mV ($n = 4$, paired t test $P < 0.005$). [Supported by NIH grants HL07101, HL27105, and HL29687 and by the NC Heart Association.]

87. Pacemaker of Rhythmic Contractions of the Enveloping Layer of the Medaka *Oryzias latipes*, a Teleost R. FLUCK, J. DeLEON,* and M. HASENFELD,* *Department of Biology, Franklin and Marshall College, Lancaster, Pennsylvania*

We reported previously (Fluck et al., 1983, *J. Exp. Zool.*, 226:245) that the enveloping layer (EVL) of the medaka embryo contracts rhythmically and that the EVL contracts into a ball when it is mechanically removed from the embryo (Fluck et al., 1984, *J. Exp. Zool.*, 229:127). Detached EVLs also contract rhythmically. We now report that rhythmic contractions do not begin until after formation of the germ ring and the embryonic shield (stage 14). The first contraction of the embryo begins opposite the embryonic shield in a region that appears to be a pacemaker for the contractions. The contractions arise in the pacemaker region and propagate across the surface of the EVL. Enveloping layer cells that overlie the embryonic shield do not appear to participate in the contractions, although these cells contract when the calcium ionophore A23187 is applied to their apical surface. We conclude that the EVL of the medaka embryo can be divided into two regions: a pacemaker region and a region that does not contract rhythmically. The behavior of detached EVLs is consistent with this conclusion. We have vitally stained small portions of EVLs with fluorescein diacetate, removed these EVLs from embryos, and recorded their contractile activity with a time-lapse video recorder. A detached EVL typically contracts into a pear-shaped ball. Rhythmic contractions always begin at the narrow end of the EVL, which corresponds to the pacemaking region of the EVL. Just as in an EVL attached to the embryo, the contractions of a detached EVL are confined to one end of the EVL. [Supported by a grant from Research Corporation.]

88. Calcium Extrusion in Cultured Heart Cells: Na-Ca Exchange vs. the Ca Pump WILLIAM H. BARRY and CARL A. RASMUSSEN,* *Cardiology Division, University of Utah School of Medicine, Salt Lake City, Utah*

The relative importance of Ca extrusion via Na-Ca exchange vs. an ATP-dependent Ca pump in regulation of cytoplasmic [Ca^{2+}] is not clearly defined. We therefore compared the effects on chick embryo ventricular cell motion (video motion detector) of abrupt exposure to 20 mM caffeine (C) in 0 Na/0 Ca (140 mM choline chloride) (Soln 1) with effects of C in 140 mM Na/0 Ca (Soln 2). All cells were exposed to 0 Na/0 Ca solution for 2 min immediately before C exposure. The results are shown below (means ± SEM, $n = 7$).

	Caffeine Contracture		Relaxation $t_{1/2}$	
	μm		s	
Soln 1	3.94±0.90	$P < 0.03$	8.60±1.22	$P < 0.001$
Soln 2	1.53±0.50		0.77±0.09	
Soln 2 plus La	2.28±0.93		6.51±2.18	

Thus, simultaneous exposure to 140 mM Na plus C resulted in a decrease in contracture amplitude and a marked increase in the rate of contracture relaxation. This effect of Na was

inhibited by exposure of the cells to 1 mM La, an inhibitor of Na-Ca exchange. Loss of ^{45}Ca from labeled cells into 0 Na/0 Ca, 0 Na/0 Ca plus C, and normal Na/0 Ca plus C was also measured at 5-s intervals, and the results are shown below (cpm lost in the first 5 s into a 0 Na/0 Ca Soln were assigned a value of 100%).

Efflux interval	5–10 s	10–15 s	15–20 s	25–30 s	30–35 s
0 Na/0 Ca	86.6	61.4	43.6	38.2	34.6
0 Na/0 Ca plus C	108.6	77.8	58.0	44.5	36.5
Normal Na/0 Ca plus C	160.6	126.9	98.0	63.0	48.2

These results suggest that Ca extrusion via Na-Ca exchange can occur more rapidly than can Ca extrusion via the Ca pump. The Ca pump appears to be a high-affinity, but relatively low-capacity, Ca transport system in these cells.

89. The Correlation of Donnan Potential Measurements in Muscle A- and I-Bands with Electrofluorochromometric Observations G. F. ELLIOTT, E. M. BARTELS,* and P. H. COOKE,* *Open University, Oxford Research Unit, Oxford, England*

In this laboratory, we have been making extensive measurements of Donnan potentials from the A- and I-bands of glycerinated and chemically skinned rabbit psoas and rat semitendinosus muscle using 3 M KCl microelectrodes (Bartels and Elliott, 1981, *J. Physiol.* [*Lond.*]., 317:85; 1982, 327:72; 1983, 343:32) and we have observed that the A-band potential falls significantly between a rigor solution without ATP and a relaxing solution containing ATP (from 5 to 2.5 mV in solutions based on 100 mM KCl). We have extended our observations to gels and threads of the A-band protein myosin and of myosin rod, and here also we observe that the potential, and therefore the protein charge, falls significantly in a solution containing ATP (Cooke et al., 1984, *Biophys. J.*, 45:7*a*, and unpublished observations). Scordilis, Tedeschi, and Edwards (1975, *Proc. Natl. Acad. Sci. USA*, 72:1325) used the fluorescent dye CC-6 to serve as an indicator of the potential measured in glycerol-extracted muscle with microelectrodes, and showed that the fluorescence decreased by ~30% on the addition of ATP. They did not then localize this effect, but Scordilis (unpublished observations), using synthetic thick and thin filaments, showed that the effect was primarily due to the myosin-containing filaments, and was moreover probably confined to the rod part of the myosin molecule (by experiments using myofibrils depleted in the myosin head fraction). Thus, there appears to be a very good correlation between the two techniques, and the time is ripe for a new optical study using high-resolution fluorescence microscopy and an appropriate potential-sensitive dye. If this could be combined with the "caged ATP" technique (Goldman et al., 1983, *Nature* [*Lond.*]., 300:701), interesting new facts about the contractile mechanism might emerge.

90. Off Gating of Calcium Release in Skeletal Muscle EDUARDO RIOS,* *Department of Physiology, Rush Medical College, Chicago, Illinois* (Sponsor: C. Schauf)

In skeletal muscle fibers, the Ca transients elicited by short (~10 ms) voltage clamp pulses keep increasing for several milliseconds after the end of the pulse. To explore the nature of this delay, we applied the absorption dye methods of Kovacs et al. (1983, *J. Physiol.* [*Lond.*]., 343:161) to record the myoplasmic [Ca^{2+}] time course and derived Ca flux from the sarcoplasmic reticulum (SR) by the procedure of Melzer et al. (1984, *Biophys. J.*, 45:637). We used a two-beam microscope/photometer apparatus that records true absorbance by monitoring incident and emergent light intensity at two wavelengths. Intramembrane charge movement was recorded simultaneously. Upon maintained depolarization, the calcium flux from the SR goes from zero through a maximum and spontaneously decreases to a much lower steady level. If the fiber is repolarized before the flux has reached its maximum, the flux keeps increasing for 2–3 ms and then falls to zero in ~7 ms. Various explanations of this delay in the off gating of the release channel were tested. The waveform of Ca flux obtained measuring [Ca^{2+}] in central regions of the fiber was compared to waveforms at peripheral regions. The release in peripheral regions turns on with less latency and turns off with no measurable delay. Therefore, the delay observed in the measurements at the center of the fiber is the time required to repolarize deep portions of the t-tubules. Within our time resolution, these results are not inconsistent with models assuming instantaneous control of the permeability of the SR Ca channel by voltage sensors in the t-tubule membrane ("plunger" models). [Supported by NIH grant AM 32808.]

INDEX TO AUTHORS OF ABSTRACTS

Abstract number follows name